CHAPTER FOUR

SYNTHETIC DERIVATIVES OF ISOOLIVIL

4.0 Introduction

In most instances, natural sources are not an economically viable way of obtaining material for commercialization. Total synthesis of bioactive compounds originally obtained from natural sources can be carried out provided the synthetic products are as active as the natural isolates. For this purpose, synthetic routes of the active compound should be explored with special reference to the yield and purity of the products obtained. However, it may be difficult to achieve economically viable synthetic routes for many drugs due to stereospecificity of activity and existence of unstable but necessary functional groups.

However, synthetic efforts of the natural compounds may be hampered by the structural complexity as in the case of vinca alkaloids or stereospecifity of binding even of simple molecules such as chloramphenicol. Thus, cultivation and fermentation under controlled conditions still remains the sources of these drugs. Indeed, there is a whole spectrum of bioactive molecules obtained through cultivation including the antimalarials artemisinin and quinine, lovastatin (antilipidemic), the anticancers taxol and captothesin and the antibiotics, tetracycline, erythromycin, rifamycins, the peptides, nystatin and griseofulvin. Nevertheless, quinine acted as an important template in the synthesis of active aromatic amino alcohols such as mefloquine,

halofantrine and lumefantrine (Folley and Tilley, 1998). The same applies to lovastatin synthetic analogs including fluvastatin (Lescol®), atorvastatin (Lipitor®) and rosuvastatin (Crestor®).

Semisynthesis, on the other hand maintains the critical functional groups during structural modification. The objectives of derivatisation of biologically active compounds are: to enhance their potency, reduce toxicity, increase spectrum of activity and improve stability. The semisynthetic derivatives of artemisinin have superior activity and pharmacokinetic parameters. Artemether, arteether, dihydroartemisinin and artesunate are the currently drugs of choice in the treatment of malaria (Jefford, 2001).

In chemical synthesis, spectroscopic and chemical methods are applied in confirming the structures of the products. The absolute structure of crystalline compounds can be obtained by X-ray crystallography under conditions that favour anomalous scattering. Chromatographic techniques e.g. TLC and HPLC are used to determine purity of the synthetic products.

4.1 Synthesis of isoolivil

Synthesis of isoolivil was first reported by Yosinori *et al.* (1996) from the corresponding substituted O-silated cyanohydrin (I), benzyl bromide (II) and but-2-enolide (III) through several steps (figure 4.1). The substance was obtained as the racemate both in solution and crystal form whereby the stereoisomers co-crystallize.

The crystal symmetry showed a monoclinic $P2_1/a$ cell of dimensions, a = 8.401(3) Å, b = 13.576(4) Å, c = 15.755(2) Å, b = 91.46°, V = 1796 $Å^3$, Z = 4 (figure 4.2). There was no solvent of crystallization observed in the crystal lattice.

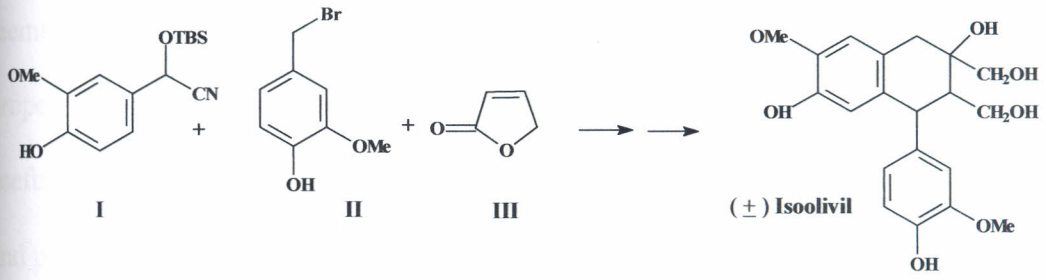

Figure 4.1: Synthesis of isoolivil (Yosinori *et al.*, 1996)

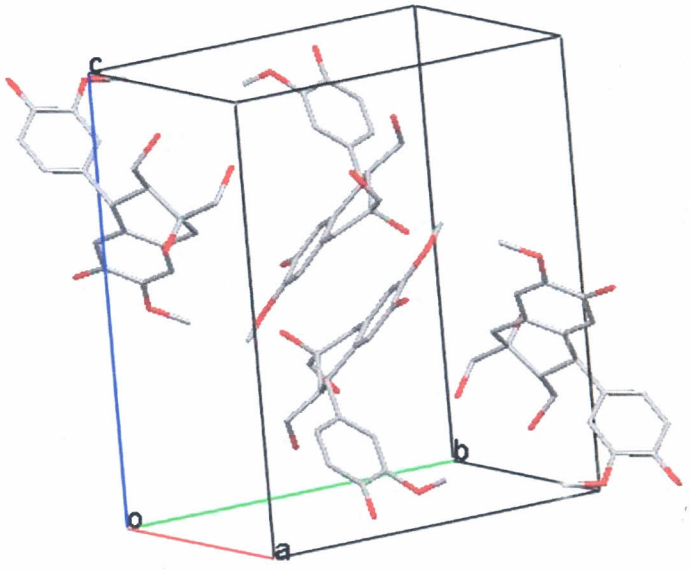

Figure 4.2: Crystal packing of racemic isoolivil (Yosinori et al., 1996)

4.2 Rationale for the derivatization of isoolivil

Isoolivil is a relatively polar compound. The polarity of the compound is conferred by the preponderance of OH groups, both alcoholic and phenolic. The latter are acidic and at physiologic pH are likely to be ionized thus hindering traversation across cell membranes. Drug action depends on pharmacokinetic and pharmacodynamic properties of the molecule and the physicochemical attributes of the ligand are very useful in drug design. The parameters affecting the biological activity were identified and parameterized by Hansch (1981) in the cerebrated equation:

$$\log (1/C) = k_1 \log P + k_2 \sigma + k_3 Es + k_4$$

where C is the concentration that reaches site of action, log (1/C) represents biological activity, log P is the partition coeficient in a water/octanol system, σ denotes the electronic parameter, Es is the Taft steric parameter descripter and $k_1 - k_4$ are constants determined by least squares regression analysis (Hansch analysis).

The polarity of a compound can be modified through appropriate derivatization with the objective of improving its pharmacokinetic parameters. Several compounds in pharmaceutical application have been subjected to derivatization to yield more potent, more stable derivatives with superior pharmacokinetic profiles. Examples of semisynthetic derivatives of common pharmaceuticals are shown in Table 4.1.

Table 4.1: **Selected semi-synthetic derivatives of pharmaceuticals in the market**

Name	Derivatives
Artemisinin	Ethers (artemeter, arteether)
	Alcohols (dihydroartemisinin)
	Ester salts (artesunate)
Erythromycin	Ethers (clarithromycin)
	Esters (erythromycin propionate)
	Azalides (azithromycin)
Tetracycline	Doxycycline, Minocycline
Lincomycin	Clindamycin
Rifamycin B	Rifampicin

4.3 Experimental

4.3.1 Reagents and materials

Dimethyl sulphate, 99% w/w (BDH Chemicals Poole, England) was used for methylation reactions. Ammonia concentrated (28% w/w) and concentrated sulphuric acid were obtained from Fischer Scientific (Loughborough, Leicestershire, UK). All other reagents were of analytical grade

4.3.2 Synthesis of di-O-methyl isoolivil

About 740 mg of isoolivil (1.973 mmol) were dissolved in 1 M NaOH (5 ml) to form an amber coloured solution. Five ml of dimethyl sulphate (52.87 mmol)were added drop wise over a period of 1 h. The reaction mixture was incubated for 3 h under constant stirring. A white precipitate was formed. The solution was quenched using 10 ml concentrated ammonia (28% w/w) to inactivate the excess dimethyl sulphate in an exothermic reaction. The reaction mixture was extracted using 100 ml chloroform. The chloroform extract was washed with 50 ml distilled water and evaporated to dryness. The weight of the residue obtained was 730 mg.

Thin layer chromatography of the reaction products was carried out on normal phase silica using ethyl acetate as mobile phase. Four spots of R_f values 0.21, 037, 0.46 and 0.63 were observed. The major spot had a similar R_f value (0.63) as the starting compound, isoolivil.

4.3.3. Column chromatography of the methylated products

The reaction products were dissolved in ethyl acetate with warming on a water bath maintained at 50 °C. The sample was loaded onto a column packed with 15 g normal phase silica. Elution was carried out using ethyl acetate as mobile phase. Sixty fractions of 5 ml each were collected. The fractions were pooled according to the TLC profile (figure 4.3). Two major fractions corresponding to the TLC spots of R_f 0.21 (fraction I) and 0.37 (fraction II) respectively were pooled and rotary evaporated to dryness. The yield for fraction I was 158.6 mg (21.7 % w/w) while that of fraction II was 60 mg (8.2 % w/w). Fraction I was composed of a mixture of isoolivil and di-O-methyl isoolivil. It was cleaned with methanol to give a white amorphous substance with a chromatographic purity of 97%, which was identified as di-O-methyl isoolivil on the basis of IR and NMR data. The compound was found to be very soluble in chloroform but poorly soluble in methanol.

Fraction II was obtained as viscous amber coloured oil. Upon HPLC analysis this fraction was found to be a mixture of three components. This fraction was therefore not worked on further due to lack of resources. Purification could be achieved through preparative HPLC with the aid of an optimized mobile phase. This fraction may have contained the methylation products of the alcoholic groups of the isoolivil molecule.

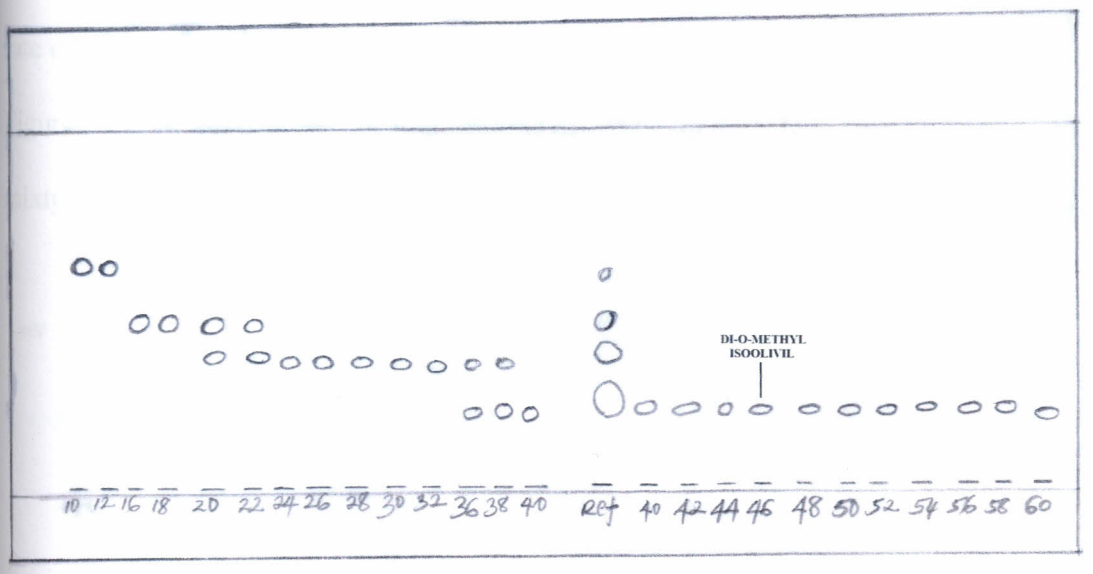

Figure 4.3: TLC profile of the column fractions of methylated isoolivil

Mobile phase, 100% ethyl acetate

4.3.4 HPLC analysis of di-O-methyl isoolivil

The compounds isoolivil and di-O-methyl isoolivil were found to have different solubility profiles in methanol and chloroform. Di-O-methyl isoolivil was found to be very soluble in chloroform, poorly soluble in methanol while isoolivil showed high solubility in methanol compared to chloroform. This showed that although the two compounds had the same TLC profile, they were not identical. Therefore the two were further investigated using HPLC.

The HPLC analysis was carried out using a Phenomenex® C_{18} column (250 x 4.6 mm) maintained at 40 °C and as mobile phase methanol-water (50:50) pumped at a flow rate of 1 ml/min. UV detection at 280 nm was used to monitor the elution of analytes. Figure 4.4 represents a chromatogram of di-O-methyl isoolivil and isoolivil in mixture. It shows that the compounds are different on account of their retention times.

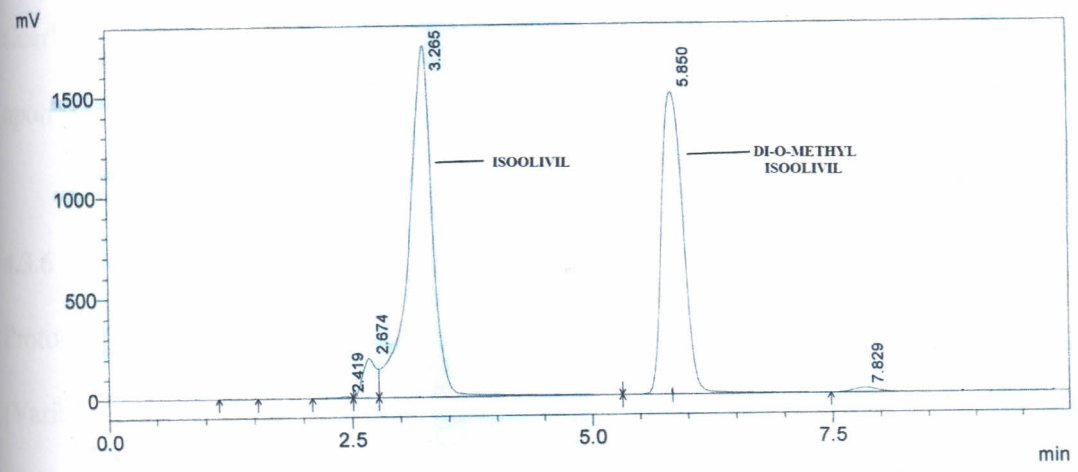

Figure 4.4: Typical chromatogram of isoolivil/di-O-methyl isoolivil mixture

Column: Phenomenex Lunar C_{18}, 250 X 4.6 mm maintained at 40 °C; Mobile phase: methanol-water (50:50)

4.3.5 Infrared analysis of di-O-methyl isoolivil

Infra red data was recorded on FT IR 8400 S (Shimadzu Corp., Kyoto, Japan) spectrophotometer operating in the transmittance mode as described under section 3.3.1. The IR spectrum obtained is shown in appendix IV. The spectrum was compared with that of the starting compound, isoolivil (appendix I). The phenolic O-H str. seen in appendix I (3485 cm^{-1}) is absent in the spectrum of di-O-methyl isoolivil

thus narrowing the alcoholic O-H band and centering it at 3300 cm^{-1}. As a result, the aromatic C-H str. band (3000 cm-1) and the adjacent C-H bands (2950 and 2800 cm^{-1}) are more prominent. The aromatic C=C vibrations generate the bands observed at1600, 1520 and 1450. The series of bands between 900 and 650 cm^{-1} (C-H wag) are further confirmation of presence of aromatic ring. The spectral differences are more distinct when the two spectra are overlaid as depicted in appendix V. Thus the IR data clearly indicates that phenolic OH groups on isoolivil were effectively methylated upon reaction with dimethyl sulphate.

4.3.6 NMR data for di-O-methyl isoolivil

Proton- and ^{13}C-NMR data was collected on a 200 MHz YH200 Varian spectrometer (Varian Inc., Paloalto, CA, USA) supported by Mercury VXWax software.

The proton NMR spectrum obtained is shown in appendix XIV (a). Twenty six protons were observed. Compared to the parent compound six extra methoxy protons were observed. The shifts for these protons are δ 3.483 (s, 3H), 3.731 (s, 3H), 3.757 (s, 3H) and 3.795 (s, 3H) as illustrated in appendix XIV (b).

The ^{13}C-NMR data for di-O-methyl isoolivil is shown in table 4.2. The carbon correlations with those of the parent compound exhibits slight differences in the chemical shifts. The confirmatory observation for the extra methoxy C-atoms are the signals at δ 55.336, 55.37, 55.473 and 55.564 which are partially resolved as shown in appendix XV (b).

Table 4.2: ^{13}C-NMR comparison data for isoolivil and di-O-methyl isoolivil

Isoolivil	Type	Carbon	Di-O-methyl isoolivil
147.48	C	C3'	149.70
145.81	C	C7	148.28
144.84	C	C4'	148.13
144.00	C	C6	147.54
137.03	C	C1'	138.65
132.17	C	C4a	132.10
125.26	C	C8a	127.51
121.91	CH	C6'	122.19
116.25	CH	C5	114.07
115.45	CH	C5'	113.53
113.51	CH	C2'	112.54
112.43	CH	C8	111.87
73.09	C	C2	73.30
68.10	CH2	C9	68.80
59.11	CH2	C10	59.93
55.78	CH3	7-OMe	55.56
55.63	CH3	3'-OMe	55.47
-	CH3	6-OMe	55.37
-	CH3	4'-OMe	55.34
45.70	CH	C3	46.70
43.18	CH	C4	43.95
38.94	CH2	C1	39.47

4.3.7 Discussion

Selective methylation of the phenolic groups of isoolivil was achieved by carrying out the reaction under mild conditions that could not cause simultaneous methylation of the alcoholic groups. Usually the alcohol OH groups react under conditions of heating the reaction mixture at about 50 °C. However, this conversion was not absolutely selective since other by-products were formed probably through methylation of some of the alcoholic OH groups. This was observed in the TLC and HPLC analysis. Presence of these impurities necessitated column chromatography in order to isolate di-O-dimethyl isoolivil.

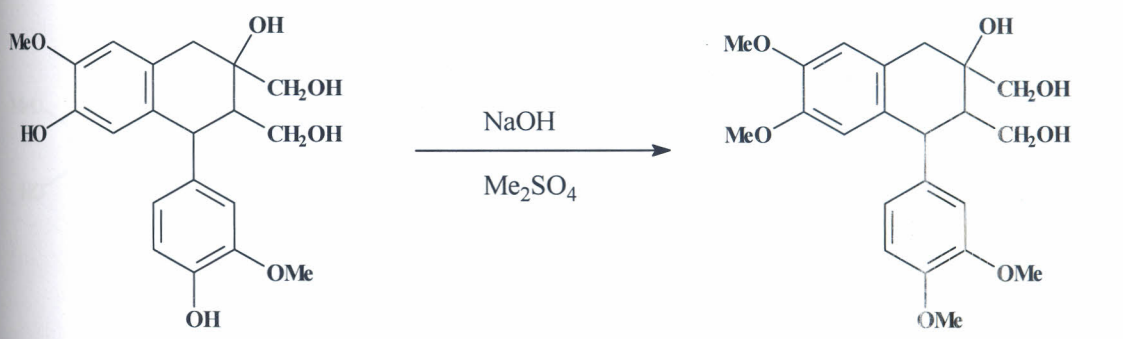

Isoolivil **Di-O-methyl isoolivil**

Figure 4.5: Synthetic scheme for di-O-methyl isoolivil

The di-O-methylated product was obtained as a white amorphous powder with melting point 186-188 °C. The melting point obtained compares well with that reported in the literature (Koerner and Vancetti, 1911). The spectral data confirmed the identity of the dimethylated derivative with the NMR showing the presence of

extra methoxy groups. The IR data showed the disappearance of the band due to the phenolic OH groups.

4.4 Oxidative cleavage of isoolivil

Oxidative cleavage at the tertiary C2-OH and primary C9-OH vicinal diol by means of lead tetra-acetate or sodium periodate was not feasible due to the unfavourable molecular conformation which is incompatible with the mechanism of reaction. The OH groups involved are oriented in the *trans* configuration so that the inter-atomic distance cannot allow the formation of the necessary cyclic intermediate. The crystal structure of the compound revealed an O1-O2 distance of 3.7 Å.

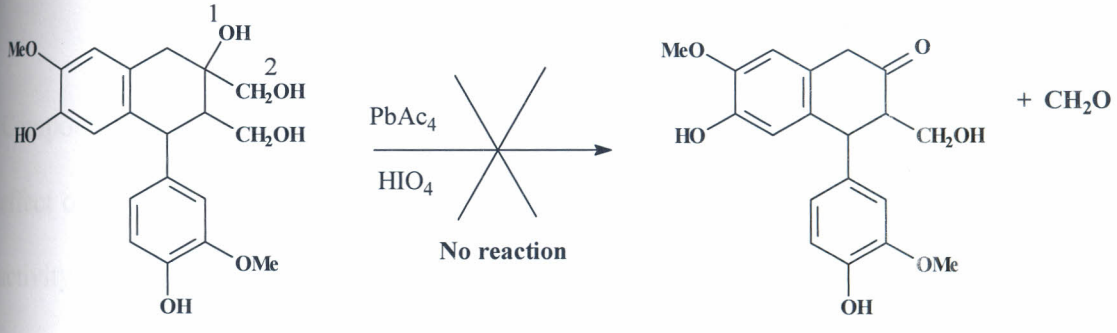

Isoolivil

CHAPTER FIVE

IN VITRO ANTIMALARIAL TESTS

5.0 Introduction

The isolation and identification of compounds from the plants under study has been described under chapters 2 and 3. Further, the derivatization of isoolivil is discussed in chapter 4. It was necessary to determine the antimalarial activities of the compounds using *in vitro* methods in order to rationalize the use of the plants *S. henningsii* and *C. abbreviata* in the treatment of malaria.

Compounds with weak antimalarial activity were derivatized in order to establish the effect of particular groups on their activity. According to the Hansch relationship the activity of drugs is a balance of the polarity and drug receptor binding (Hansch, 1981). The former is closely related to the ability to undergo absorption and to traverse cell membranes.

In vitro studies offer a good model for assessing the biological activity of molecules. However, the results need to be confirmed *in vivo* to justify further development of the molecules. In some instances, inactivity *in vitro* does not rule out *in vivo* activity. This

is especially true in cases were the active entities are the metabolites or where the metabolites are active as well.

5.1 The role of *in vitro* tests in phytochemical research

Administration of drugs to humans before establishing their safety is against ethical practice. The most important aspects during drug development include efficacy, acute and chronic toxicity and clinical trials. Initial studies are based on *in vitro* and animal models before confirming the activity in man.

Claims on the activity of plant extracts are first subjected to *in vitro* scrutiny before further research in undertaken. Drug development is an expensive exercise which is not worthy pursuing if the chances of success are limited. This makes it necessary to drop any candidate molecules that might not end in the market. Consequently, a lot of investment and research has over the years been directed to validating the activities observed in order to increase chances of success. One of the most significant outcomes of these efforts is the high throughput screening which highly depends on *in vitro* tests.

High throughput screening depends on computerization, miniaturization and robotics. It is applicable in the testing of synthetic molecules and enables combinatorial syntheses in drug development. The operating principle is to have as many molecules as possible fail in the initial stages so that few of them continue in the development line.

5.2 *In vitro* antimalarial tests

The malaria parasites are fastidious organisms requiring growth conditions closely similar to the natural environment. As a result, *in vitro* culture medium incorporates human serum, red blood cells in addition to the RPMI-1640 medium. The optimal conditions were described by Trager and Jensen (1976) using *P. falciparum* isolated from the *Aortus trivirgatus* monkey.

For antimalarial tests, the samples are dissolved in inert solvents such as water, methanol or dimethylsulphoxide (DMSO) and incubated with the parasitized RBCs. After 72 h, the viability of the malaria parasite is determined using established methods. The activity of the samples against the parasite is compared to that of a standard antimalarial drug such as chloroquine, artemisinin or quinine.

Desjardins *et al.* (1979) described a method based on the inhibition of the uptake of ^{3}H-hypoxanthine by *P. falciparum*. During the experiment, test substances are incubated with the parasites and interrupted after 24 hours for the addition of the tritiated hypoxanthine. Erythrolysis is achieved through freezing and the parasites harvested by filtration. The radioactivity incorporated into the parasites is determined by means of scintillation. The IC_{50} values are estimated using a suitable computer program.

In 1993, Makler *et al.* described a protocol, which measures the parasite lactate dehydrogenase (pLDH) activity of the parasites after exposure to the test substances. For this purpose the parasitized RBCs are incubated with the test substances under conditions of normal growth for 72 hours. The cells are lysed through freeze- thaw and the pLDH activity evaluated spectrophotometrically in a mixture of nitro blue tetrazolium (NBT), phenazine ethosulphate (PES) and Malstat™ reagent. The optical density is read by means of a microplate reader at 650 nm. The IC_{50} is calculated by comparing the optical activity with that of untreated controls.

5.3 Experimental

5.3.1 Reagents and Materials

Malstat™ reagent for the *in vitro* assessment of antimalarial activity was purchased from Flow Incorp. (Oregon, PA, USA). The RPMI-1640 medium for the maintenance of parasite cultures was obtained from Gibco/BRL Life Technologies (Gaithersburg, MD, USA). Nitro blue tetrazolium and phenazine ethosulfate (Sigma Chemical Company, St. Louis, MO, USA) were used for the color development during the assay.

Sterile cellulose acetate filters (0.2 μm) were used for the sterilization of the culture media. All plastic and glassware used were sterile and singly packed. The gas mixture (90% nitrogen, 5% oxygen and 5% carbon dioxide) for maintenance of cultures was prepared by the BOC Gases, Kenya according to specifications.

5.3.2 Equipment

A 96-channel EL800 Universal Microplate Reader (Bio-Tek Instruments Inc., Vinooski, VT, USA) was used for measurement of the absorbance of the microtiter assay plates. An IEC Centra CLD centrifuge (International equipment Co., UK) was used for the isolation of RBCs and all centrifugation experiments while a CellHouse 170 incubator (RS Biotech, Irvine, Scotland) was employed in the incubation of parasite cultures and test preparations. A Nikon microscope was used for monitoring of the parasite cultures and determination of parasitemia.

5.3.3 Malaria parasites

The parasites used for *in vitro* work included the chloroquine sensitive D6, chloroquine resistant W2 and multidrug resistant V1/S strains of *Plasmodium falciparum*. They were a kind donation from the Kenya Medical Research Institute , Nairobi and the Wellcome Trust laboratories, Nairobi, Kenya.

5.4 Preparation of solutions

D-Sorbitol 5%: Into 5 g D-sorbitol were added 6.7 ml PBS and the solution made to 100.0 ml with distilled water. It was sterilized using the cellulose filters.

NBT stock solution: An aqueous solution of 100 mg NBT was prepared in a 50 ml plastic centrifuge tube externally lined with aluminium foil with the aid of vortexing. The NBT solution was stored in the dark at 4° C until use.

PES stock solution: About 5 mg of PES were dissolved in 50 ml distilled water in a 50 ml sterile centrifuge tube. This solution was dispensed into 5 x 15 ml centrifuge tubes and stored at -20° C until use.

5.5 Preparation of stock RPMI-1640 culture medium

One litre of distilled water was transferred into a flat bottomed flask. HEPES, 5.94 g, together with 2 g glucose and 10.4 g RPMI-1640 powder were dissolved in the water with the aid of magnetic stirring before making the volume to 1130 ml with water. The pH of the medium was adjusted to 7.2 using 20 % w/v sodium hydroxide.

5.6 Red blood cells

Blood was collected from consenting donors with group O-positive. The blood was withdrawn sterile blood bags containing acid-citrate-dextrose anticoagulant of composition tris-sodium citrate 22 g, citric acid 8 g, dextrose 24.5 g per litre of solution. It was placed upright in the refrigerator at 4 °C overnight for the blood cells to settle. The plasma was expressed and 5 ml aliquots the blood cell concentrate transferred into 15 ml centrifuge tubes and centrifuged at 2000 rpm for 5 min. The supernatant and the white blood cells layer was aspirated off. The RBCs were washed three times using 10 ml RPMI stock solution by alternate shaking, centrifugation and

aspiration cycles. To make 50 % hematocrit an equal volume of RPMI stock solution was added.

5.7 Preparation of serum

Blood was collected from consenting donors in blood bags without anticoagulant and left overnight to clot and thereafter placed in the deep freezer (-20 °C) for 3 h. The blood bag contents were thawed and the serum decanted into 50 ml centrifuge tubes. The serum was centrifuged at 3000 rpm and decanted into a second set of 50 ml centrifuge tubes and inactivated in an equilibrated water bath maintained at 56 °C for 30 min. The inactivated serum was transferred into 15 ml centrifuge tubes and stored at -20 °C.

5.8 Preparation of complete culture medium

The complete culture medium was prepared by mixing 85.8 ml of the RPMI stock solution with 4 ml $NaCO_3$ solution (5% w/v), 0.2 ml gentamicin for injection (5% w/v), 10 ml human serum. The mixture was sterilized by filtration on a 0.2 μm membrane filter.

5.9 Preparation of 50% hematocrit suspension

Twenty ml of freshly withdrawn whole blood were placed in four sterile centrifuge tubes and centrifuged at 2000 rpm for 5 minutes. The supernatant and the WBC buff layer were aspirated off. The RBCs were washed three times using 10 ml RPMI-1640

stock solution with centrifugation and aspiration of the supernatant. An equal volume of RPMI-1640 stock solution was added to make 50% HCT.

5.10 Malaria parasite culture

5.10.1 Initiation of cultures

The cultures were initiated using parasites previously cryopreserved under liquid nitrogen. The vial containing containing 0.5 ml of cells was quickly thawed by shaking gently at 37° C in a water bath. The cells were aseptically transferred into a 15 ml centrifuge tubes and of 3.5% sterile sodium chloride (0.7 ml per 1.0 ml of PRBC) added drop wise. Further, 5 ml of CRPMI were added and mixed. The mixture was centrifuged at 2000 rpm for 5 min and the supernatant pipetted off.

The cells were transferred into a 75 ml culture flask and re-suspended in 5 ml complete media before adding 0.05 ml RBCs to bring the hematocrit to 5%. The culture was aerated with the gas mixture and incubated at 37 °C. Media was changed until the parasites adapted and thereafter every two days.

5.10.2 Maintenance of growing cultures

Parasite cultures were subjected to daily media change by carefully aspirating the media without touching the cells, adding fresh 5 ml CRPMI, aerating the flask and incubating at 37 °C. Parasitemia was monitored microscopically using a Giemsa stained blood smears

5.10.3 Subculture of PRBC

The growing culture was transferred into a 15 ml centrifuge tube and spun at 2000 rpm. The media was aspirated and a smear prepared, stained using 3% Giemsa stain solution and the percentage parasitemia determined. Meanwhile, the PRBCs were diluted with 2.5 ml of culture medium and incubated at 37 °C.

The volume of the suspension required to give a parasitemia of 5% was worked using the parasitemia obtained with the stained slides. After dilution of the parasite suspension in the new culture flask, 0.1 ml of RBCs was added to achieve 5% hematocrit and a final volume of 5 ml. The sub culture was maintained as described in section 5.10.2.

5.11 *In vitro* antimalarial tests

5.11.1 Preparation of the test substances

The drugs under test were dissolved in methanol or DMSO as appropriate and diluted in the CRPMI to the desired concentration. The methanol concentration was kept at 0.1% v/v in the final concentration in the first well. Figure 5.1 represents the dilution scheme for the extracts and pure compounds under test.

Dilution	Diluent	Extract	Pure
Stock solution	Methanol	50 mg/ml	20 mg/ml
		↓	↓
100 µl → 1 ml	Sterile purified water	5 mg/ml	2 mg/ml
		↓	↓
200 µl → 1 ml	Sterile purified water	1 mg/ml	400 µg/ml
		↓	↓
500 µl → 1 ml	CRPMI	500 µg/ml	200 µg/ml
		↓	↓
50 µl into well	CRPMI	250 µg/ml	100 µg/ml

Figure 5.1: Dilution scheme for the test substances

5.11.2 Incubation of test substances with PRBC

The antimalarial tests were carried out when the parasites were at the ring stages. The parasitemia was adjusted to 5% before the test. The PRBC and RBC suspensions were diluted to 2 % hematocrit. The 96-well microtitre plate was designed to as shown in figure 5.2.

	1	2	3	4	5	6	7	8	9	10	11	12
A	→	D1								↓	↓	RBC
B	→	D1								STD	STD	RBC
C	→	D2								STD	STD	RBC
D	→	D2								STD	STD	RBC
E	→	D3								STD	STD	PRBC
F	→	D3								STD	STD	PRBC
G	→	D4								STD	STD	PRBC
H	→	D4								STD	STD	PRBC

Figure 5.2: Design of the 96-well microtitre plate used for antimalarial tests

D – Test drug, STD – Standard drug, RBC – Unparasitised red blood cells,
PRBC - Parasitised red blood cells

To each well were added 50 µl of CRPMI. The drug solutions (50 µl) were added into the first well and a 1:2 serial dilution was performed to 9-dose levels in duplicate. At the end of the dilution series, the last 50 µl were discarded. The PRBC suspension (200 µl) was added to each well except the wells designated for RBC suspension (A12-D12). The RBC suspension (200 µl) was added at 2% hematocrit. The solutions were aerated with the gas mixture and incubated in a humidified gas chamber maintained at 37 °C for 72 hours. The reaction was stopped by freezing the plates which was also designed to hemolyse the RBCs. All antimalarial assay experiments were carried out on duplicate plates.

5.11.3 Malstat™ assay

The microtitre plates were thawed at room temperature for about 1 h at room temperature. Onto a second plate were transferred 100 µm of Malstat™ reagent per well followed by 20 µl of the PRBC, RBC and compound in the respective wells. The PRBC and RBC were prepared at 2% hematocrit.

Meanwhile the NBT (2 mg/ml) and PES (0.1 mg/ml) solutions (section 5.3.2) were mixed at a ratio of 1:1 and 20 µm of the mixture were added to the hemolysed parasite/Malstat suspension. The plates were wrapped with aluminium foil and incubated for 2 hours in the dark at room temperature. The optical density of the assay plates were read spectrophotometrically at 650 nm using the Universal Microplate Reader. The results obtained are recorded in table 5.1.

5.12 Data Analysis

The absorbance values obtained were treated to mathematical manipulation to give the percentage inhibition of parasite growth. The IC_{50} was estimated from the inhibition trends for the individual test substances. The percentage inhibition was computed according to equation 5.1.

$$\textbf{Percentage inhibition} = 100 - \left[\frac{\textbf{OD (TEST) - OD (RBC)}}{\textbf{OD (PRBC) - OD (RBC)}} \textbf{X 100} \right] \quad \ldots\ldots\ldots (5.1)$$

Where OD is the optical density and TEST represents the test substance or standard drug. The IC_{50} values were estimated by plotting log-dose response curves using MS-Excel 2003.

5.13 Antimalarial activity of extracts

Table 5.1 is shows the IC_{50} values for the methanol extracts of *Strychnos henningsii* root and crude fractions derived thereof against the W2 and V1/S strains of *P. falciparum*.

Table 5.1: IC_{50} values for *Strychnos henningsii* extracts

Extract/fraction	IC_{50}, µg/ml (W2 strain)	IC_{50}, µg/ml (V1/S strain)
Methanol extract (ME)	25.1	8.9
MEA	56.2	12.6
MWEA	39.8	39.8
Artemisinin	0.032	0.011

MEA – ethyl acetate fraction, MWEA - ethyl acetate extract of the water fraction (alkaloids).

The results obtained show that the antimalarial activity of the methanol extract (ME) had equal contribution from the alkaloids (MWEA) and non-alkaloidal components (MEA). Furthermore, activity of the methanol extract decreases upon fractionation such that MWEA and MEAhave higher IC_{50} values.

5.14 Antimalarial activity of pure compounds

Table 5.2 represents the IC_{50} values for the pure lignans isolated from the methanol extract of *Strychnos henningsii* root against the W2 and D6 strains of *P. falciparum*. The compounds were compared with the standard drug chloroquine.

Table 5.2: IC_{50} values for isolates from *Strychnos henningsii*

Compound	IC_{50}, µg/ml (W2 strain)	IC_{50}, µg/ml (D6 strain)
Isoolivil	25.1	0.39
Henningnol	89.1	0.94
Di-O-methyl isoolivil	141.2	1.20
Chloroquine	0.0224	0.00158

W2 – Chloroquine resistant *P. faciparum*, D6 - Chloroquine sensitive *P. faciparum*.

According to the results obtained, isoolivil depicted the highest antimalarial activity compared to the henningnol and di-O-methyl isoolivil against the two parasite strains tested. The IC_{50} of isoolivil was about 4 times that of henningnol for the W2 and thrice for D6. Similarly, the dimethyl derivative of isoolivil was almost 6 times less active than the parent compound against W2 and 41 % as active against D6.

There are significant chemical structural differences between isoolivil and henningnol which would account for the differences in activity. Isoolivil consists of an aryl-substitued tetrahydronaphthalene skeleton while henningnol is a di-aryl substituted

tetrahydrofuran. This structural divergence gives rise to conformational differences which affects molecular properties that depend on conformation (figure 5.3). These include crystallization and drug-receptor interaction. The phenyl ring in isoolivil lies approximately perpendicular to the fused tetrahydronaphthalene thus creating a groove. While both phenyl rings in henningnol rest on the same plane mutually perpendiclar to the tetrahydrofuran ring. The effect of this conformation on polymorphism of isoolivil is discussed in section 3.4.2. Its impact on antiplasmodial activity is clearly seen in the IC_{50} values obtained (table 5.2).

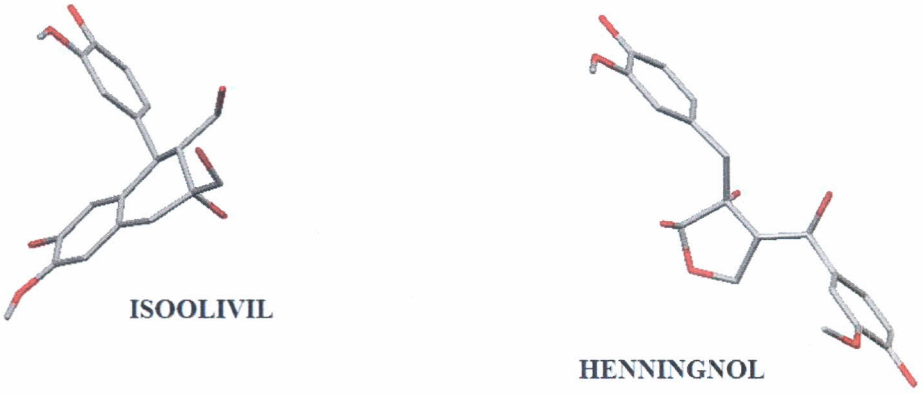

Figure 5.3: Conformational differences between isoolivil and henningnol

It appears that etherification of the phenolic groups of isoolivil as in di-O-methyl isoolivil, drastically reduces activity of the compound (table 5.2). This implies that free phenolic OH is required for activity. These OH groups could be involved in receptor binding probably by H-bonding, a property that is lost with etherification.

5.15 Discussion

Absorbance values obtained are a measure of the viability of the *Plasmodium falciparum* parasites after incubation with the drugs. The pLDH catalyses the reaction of NBT and PES to form formazan complex whose absorbance is determined at 650 nm. Thus, the absorbance observed is related to the pLDH content and parasite viability.

$$\text{NBT} + \text{PES} \xrightarrow{\text{pLDH}} \underset{(650\ \text{nm})}{\text{FORMAZAN COMPLEX}}$$

The method presents a convenient way of estimating activity of test compounds against the malaria parasite. Being a spectrophotometric method it is easy to perform and uses cheaper equipment. The procedures are safe and relatively faster to perform. The alternative method which makes use of ^{3}H-hypoxanthine, suffers the disadvantage of employing radioactive components that which requires extra safety measures for protection against the radiation related side effects. However, some of the procedures are delicate and require extra precaution especially the incubation of the test mixtures under dark conditions. The dilution procedures also need to be accurate for consistency of results.

The extracts and compounds tested during the study showed weak activity against the chloroquine resistant W2 strain while activity was drastically improved for the sensitive D6 strain. This could imply that active compounds share the same

mechanism of resistance of the parasite to chloroquine. This should be further investigated at the molecular level.

The most active among the purified lignans tested was isoolivil against both strains of the parasite. The compound may possess the optimal topochemical requirements for drug-receptor binding thus rendering henningnol less active due to structural differences. Further, the methyl derivative of isoolivil showed reduced activity compared to the parent compound. The free phenolic groups are therefore required for activity probably by participating in drug-receptor interactions.

The activity recorded of the individual pure components cannot account for the use of *S. henningsii* in malaria treatment. Chloroquine was far more active against the parasites than isoolivil. It was further observed that activity of the methanol extract reduced upon fractionation (section 5.13). In addition the alkaloids holistiine and holistiline isolated from *S. henningsii* have been shown to weakly active (Wright *et al.*, 1994). The various components of the plant may be exerting a synergistic or additive antiplasmodial effect. This means that in principle the crude extracts of *S. henningsii* are more useful as antimalarials than the pure compounds.

CHAPTER SIX

GENERAL DISCUSSION AND CONCLUSION

The plants under study *Cassia abbreviata* Oliv. and *Strychnos henningsii* Gilg., were chosen on the basis of folklore among the Taita community. Knowledge on the use of the plants for malaria treatment is not exclusive to herbalists but general within the community. This means that access to the treatment attracts no cost, thus making it an attractive choice for the patients. Socio-economic factors dictate that most communities living in remote areas of Kenya use herbal remedies which are part of their heritage. It is evident that these Traditional medicines have shown efficacy over the years. However, success of treatment heavily relies on the correct diagnosis which may not be possible under traditional setups due to limited diagnostic knowledge and facilities among the traditional practitioners. This problem should be addressed through integration of traditional medical practice into the healthcare system functioning in complementarity with the conventional medicine. This model has been successfully applied in Tanzania. In Kenya, there is urgent need to enact legislation that controls the practice of traditional medicine to ensure ethical practice. This will enable to Ministry of Health to harness the benefits of traditional medicine for the comprehensive health of the society.

In Kenya, herbalists still rely on natural sources for their medicines. However, due to population explosion and increased agricultural and other economic activities, exploitation of this resource is not sustainable. There is imminent danger of deforestation and destruction of biodiversity. Hence the need to intensify conservation campaigns through conservative harvesting and cultivation of the medicinal plants. This is especially important for the plants studied since it is the roots are used for malaria treatment. The relevant government departments, researchers, provincial administration, religious groups, pressure groups and other suitable organs need to educate the people on conservation of biodiversity. Cultivation of medicinal plants should be emphasized since it can be made a mainstream economic activity.

The primary objective of cultivation of medicinal plants is to ensure sustainable harvesting. This is in line with the Convention on Biological Diversity (CBD) guidelines on conservation of species and environmental integrity. This would contribute towards optimization of the growth conditions and dosage standardization of the medicinal plant material. Commercial cultivation is the source of the antimalarials quinine *(Cinchona spp)* and artemisinin *(Artemisia annua)*. The 21st century has seen increased demand for natural medicines and alternative therapies. Popular herbs including *Panax ginseng*, *Hypericum spp*, *Oenothera biennis* (evening primrose), *Allium sativum* (garlic), *Zingiber officinale* (ginger), are obtained through cultivation.

Traditional African medicine is considered primitive and ineffective by some orthodox practitioners. In addition, the safety and efficacy of herbal preparations is a matter of concern for many scientists, health workers and regulatory authorities. However, it should be noted their long history of use confirms their efficacy (Elujoba *et al.*, 2005). These medicines are unique because they exert multiple pharmacology and the observed effects are the additive or synergistic activity of numerous components. In some cases the crude product extracts have better activity than the pure isolates (Saxena *et al.*, 2003). Despite scepticism herbal medicines have gained popularity and are currently multibillion dollar business endeavours (Barnes *et al.*, 2004). Furthermore, it is estimated that over 80% of people living in the developing countries rely on traditional medicine due to poverty (Patwardhan *et al.*, 2004).

In accordance with objectives, the plants under study were worked on with the view of isolating pure antimalarial components. Several strategies were adopted to effect isolation. Water/organic solvent partitioning was applied as a clean up process prior to column chromatography. Generally, the polar components that were extractable into water were not worked on due to resource constraints. However, it is recognized that these components may have a significant contribution towards the antimalarial activity of the plants considering that traditionally it is the decoction that is used for treatment of malaria.

Partitioning of the methanol extract in ethyl acetate/water solvent system afforded separation of the alkaloids from the non-alkaloidal components. The non-alkaloids

were extracted into the organic layer while the alkaloids remained in the aqueous layer probably in the salt form. This was a critical event which allowed for the isolation of the lignans and triterpenoids without interference from the alkaloids. The ethyl acetate fraction was subjected to a column chromatography work up to yield the lignans isoolivil and henningnol and the triterpenoid epifriedelinol. This is the first report of lignans from *S. henningsii*. Furthermore, henningnol is a novel lignan described for the first time. This compound was characterized using X-ray crystallography and spectroscopic data.

The methanol extract of *S. henningsii* has been reported to be active against the malaria parasite. Antimalarial activity was also observed in the ethyl acetate fractions containing alkaloids and non-alkaloids. In previous studies, the alkaloids holistiine and holistiline have been shown to possess weak antimalarial activity (Wright *et al.*, 1994; Friederich *et al.*, 1999). Consequently, the present study focussed on the non-alkaloidal components in order to establish their contribution to the antimalarial activity of the plant. These compounds showed activity against the chloroquine sensitive *P. falciparum* strain, D6. The activity of the plant is probably due to the additive or synergistic effects of alkaloids and lignans. In addition Strychnos alkaloids retuline and isoretuline have been shown to elicit antinflammatory, analgesic and antispasmodic activities (Tits *et al.*, 1991). This contributes greatly into alleviating the malaria symptomatology in addition to parasitemia clearance. It clearly demonstrates the benefits of the multiple pharmacological effects exerted by plant extracts.

Isoolivil was obtained in high yield thus permitting derivatization. The isolated substance was used for derivatization since it was not possible to carry out total synthesis of isoolivil due to resource limitations. It was reasoned that the polarity of isoolivil may limit its antiplasmodial activity. Chemical modification was aimed at improving on the lipophilicity of the compound and determining the effect on its activity. Towards this end, the phenolic OH groups of isoolivil were methylated using dimethyl sulphate. The di-O-methylated derivative was found to be less active against *P. falciparum* compared to the parent compound.

The methanol extract of *Cassia abbreviata* has been reported to be active against *P. falciparum* (Connelly *et al.*, 1996; Weenen *et al.,* 1990). Chemical tests showed that the extract contained phenolic compounds. Flavonoids have previously been reported from the plant. The bark is also known to contain tannins. This extract was not worked on further. However, the chloroform extract yielded ß-sitosterol and chrysophanol both of which have been reported from the plant (Mutasa and Kahn, 1995)

All the isolates were identified mainly using X-ray crystallography since they were crystalline. This permitted the observation of polymorphism with isoolivil. Three new polymorphs of the compound were described for the first time namely, the ethyl acetate solvate, acetonitrile-water solvate and the hemihydrate. The crystal structure of the novel lignan henningnol was worked out. Further, a new crystal structure for ß-sitosterol, the hemihydrate was also encountered in contradistinction with the monohydrate described in the literature.

The study provided further knowledge regarding the phytochemistry and antiplasmodial activity of *Cassia abbreviata* and *Strychnos henningsii*. The results obtained rationalize the use of *Strychnos henningsii* for the treatment of malaria among the Taita. The lignans isolated need to be tested *in vivo* using *Plasmodium bergei* in the mouse model. The compounds may show increase or decrease in *in vivo* activity depending on the influence of metabolism and other pharmacokinetic factors.

Further work needs to be carried out to isolate and structurally characterize more compounds from the two plants. The aqueous fraction of *Strychnos henningsii* should be worked on to isolate the polar water soluble components. No glycosides for instance have been reported from the plant. In addition there may be phenolics and sugars in this fraction. Some of these polar compounds may possess antiplasmodial activity

The methanol extract of *Cassia abbreviata* needs to be fractionated on Sephadex® in order to isolate the phenolics. These compounds should be tested for antiplasmodial activity. There is no report in the literature of antiplasmodial tests of the pure isolates from the plant.

REFERENCES

Achenbach H., Waibel R. and Addae-Mensah I. (1983). Lignans and other constituents from *Carissa edulis*. *Phytochemistry* 22 (3), 749-753.

Anderson R.A., Knols B.G.J. and Koella J.C. (2000). *Plasmodium falciparum* sporozoites increase feeding associated mortality of their mosquito hosts *Anopheles gambiae* s.l. *Parasitology* 120, 329-333.

Angenot L. and Tits M. (1981). Isolation of a new alkaloid (O-acetylretuline and a triterpenoid (friedeline) from *Strychnos henningsii* of Zaire. *Planta medica* 41, 240-243.

Arrow K.J., Panosian C. and Gelband H. (eds.). (2004). Saving lives, buying time: economics of malaria drugs in age of resistance. The National Academy Press, Washington D.C., USA. pp 130-131.

Azas N., Laurencin N., Delmas F., Di Giorgio C., Gasquet M., Laget M., and Timon-David P. (2002). Synergistic *in vitro* antimalarial activity of plant extracts used as traditional herbal remedies in Mali. *Parasitol. Res.* 88, 165-171.

Barnes P.M, Powell-Griner E., McFann K. and Richard L. N., (2004). Complementary and Alternative medicine use among adults: United States, 2002. *Advance Data.* 343, 1-20.

Beentje H.J. (1994). Kenya trees, shrubs and lianas. National Museums of Kenya. Nairobi, Kenya. pp 239, 465.

Benoit-Vical F., Valentin A., Cournac V., Pélissier Y., Mallié M. and Bastide J. (1998).In vitro antiplasmodial activity of stem and root extracts of *Nauclea latifolia* S.M. (Rubiaceae). *J. Ethnopharm.* 61, (3), 173-178

Betteridge P. W., Carruthers J. R., Cooper R. I., Prout K.& Watkin D. J. (2003). CRYSTALS version 12: software for guided crystal structure analysis. *J. Appl. Cryst.* 36, 1487.

Bousema J.T., Gouagna L.C., Meutstege A.M., Okech B.E., Akim N.I.J., Githure J.I., Beier J.C. and Sauerwein R.W. (2003). Treatment failure of pyrimethamine-sulphadoxine and induction of *Plasmodium falciparum* gametocytaemia in children in Western Kenya. *Trop. Med. Int. Health* 8(5), 427-430.

Bowen M.F. The sensory physiology of host seeking behaviour in mosquitoes. *Ann. Rev. Entomol.* 36, 139-158.

APPENDIX I: IR SPECTRUM OF ISOOLIVIL

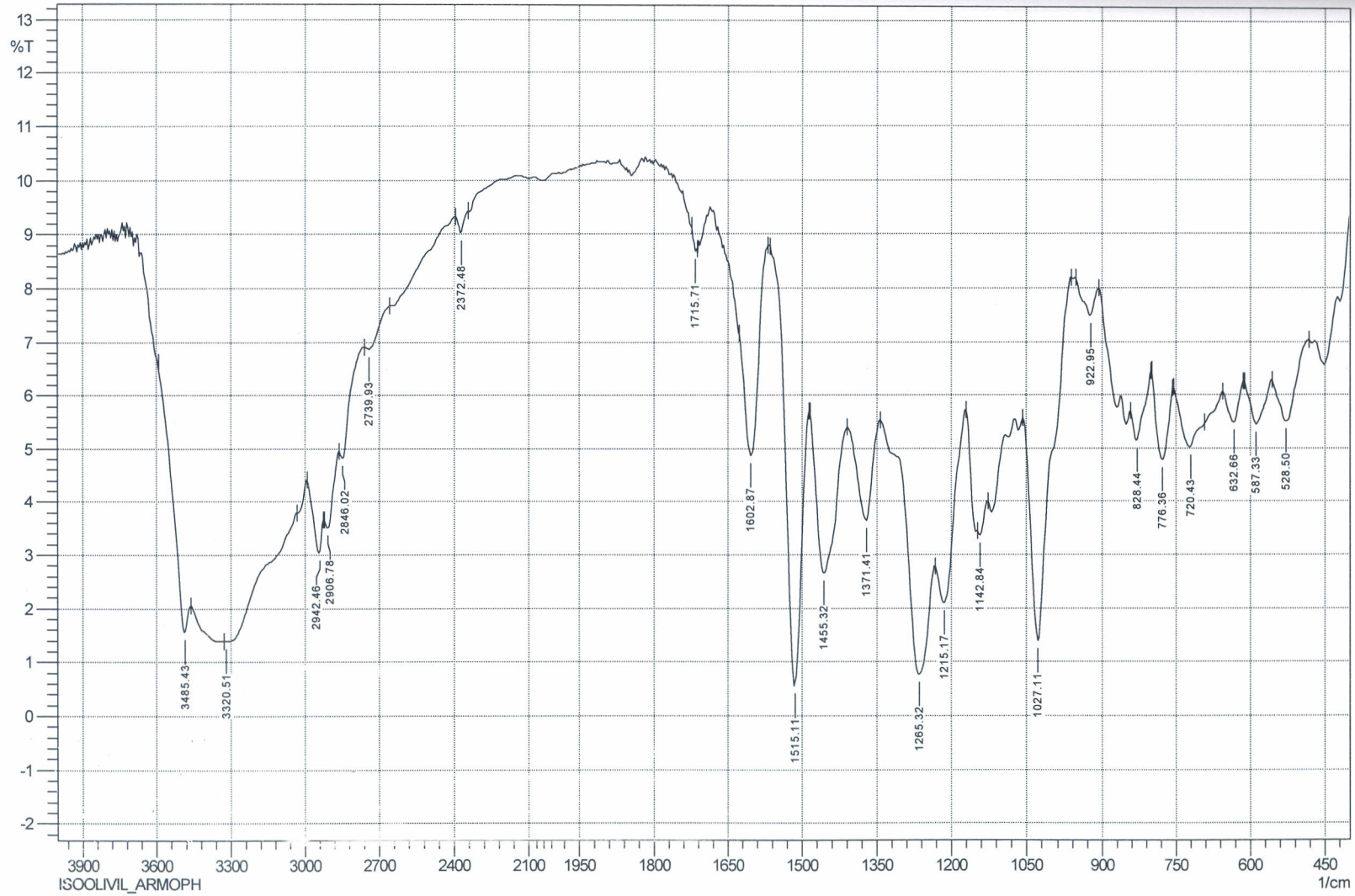

APPENDIX II: IR SPECTRUM OF EPIFRIEDELINOL

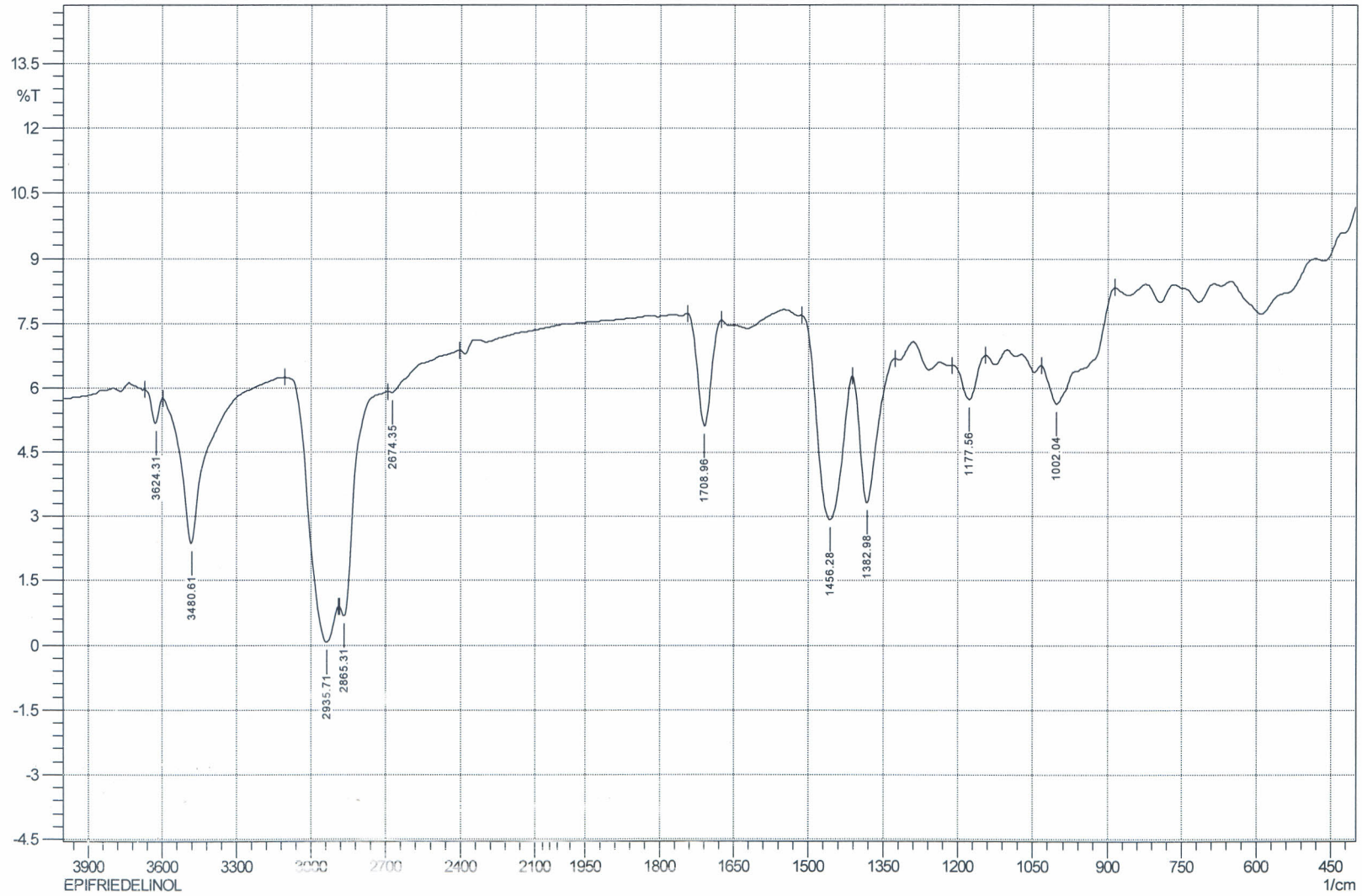

APPENDIX III: IR SPECTRUM OF HENNINGNOL

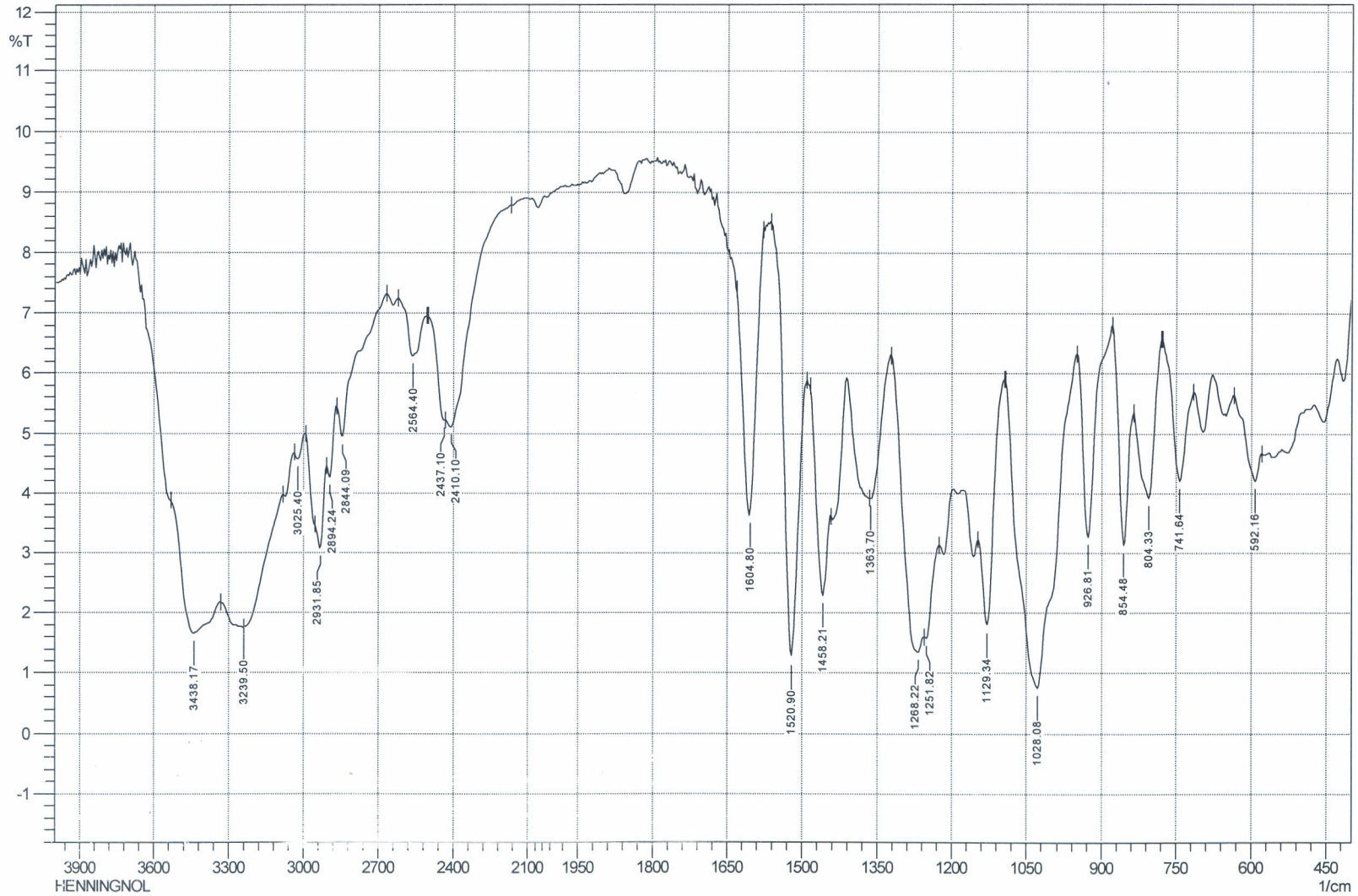

APPENDIX IV: IR SPECTRUM OF O-DIMETHYL ISOOLIVIL

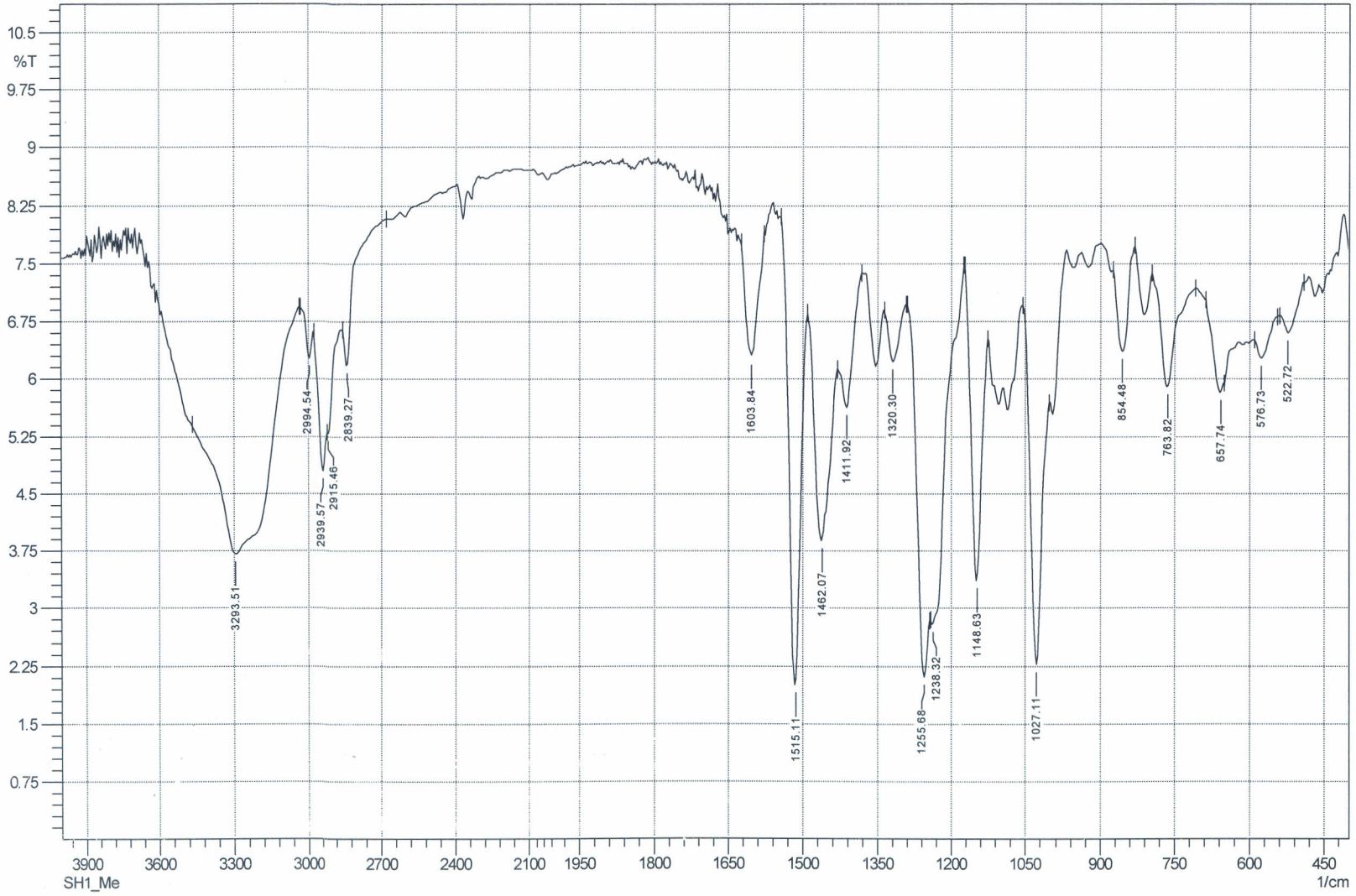

APPENDIX V: OVERLAY OF THE IR SPECTRA OF ISOOLIVIL AND O-DIMETHYL ISOOLIVIL

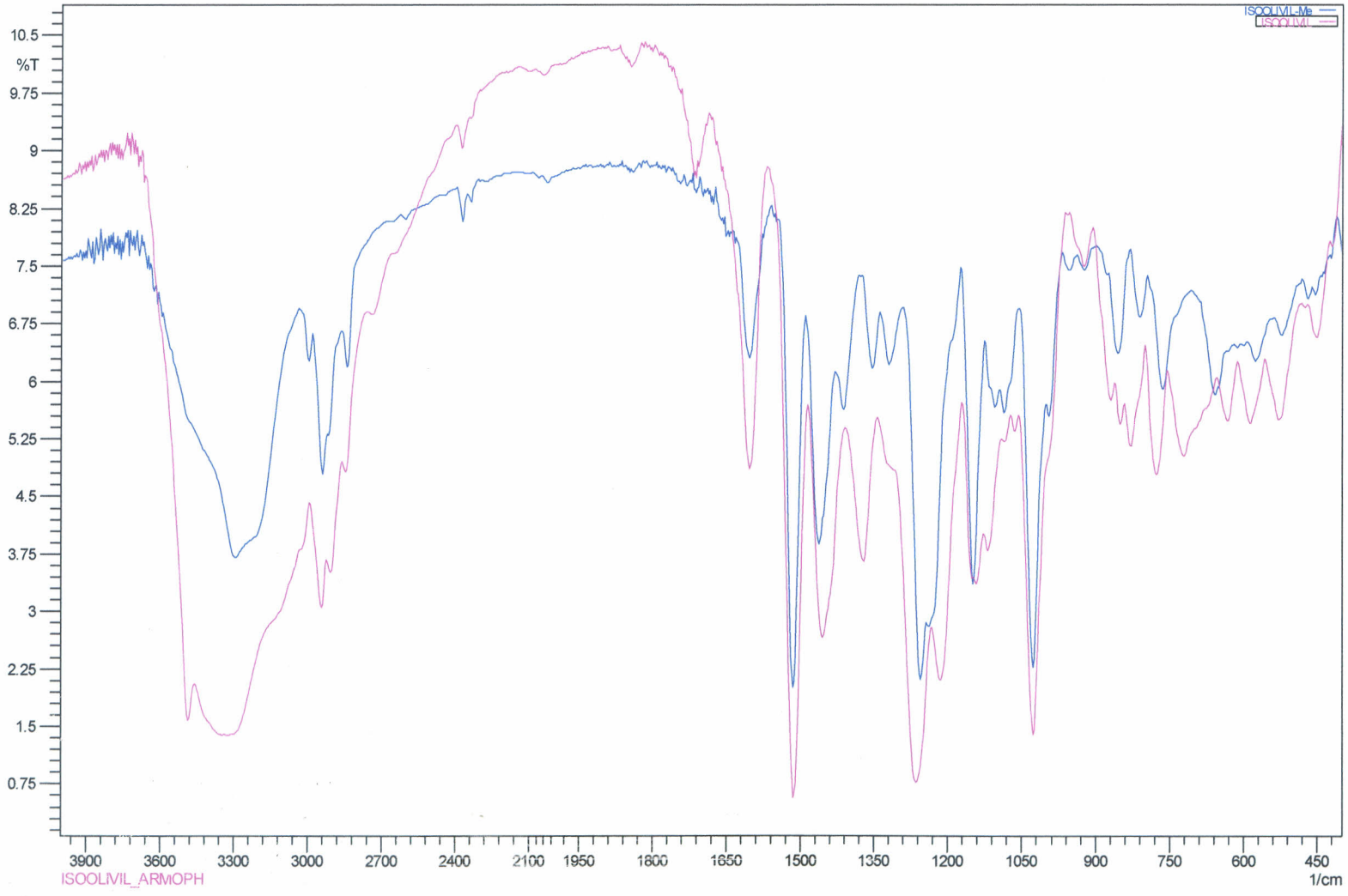

APPENDIX VI: ^{1}H-NMR SPECTRUM OF HENNINGNOL

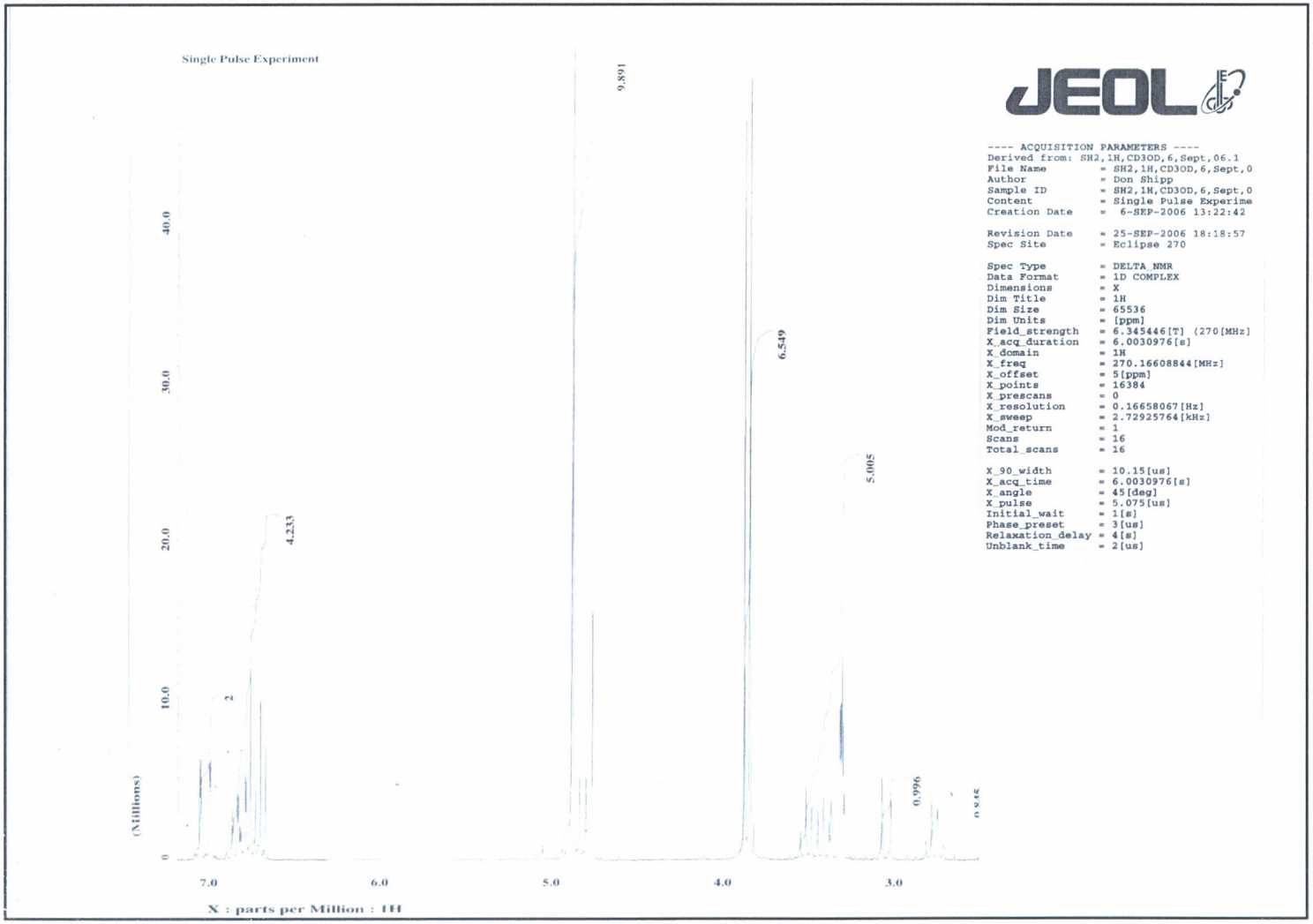

APPENDIX VII: ^{13}C-NMR SPECTRUM OF HENNINGNOL

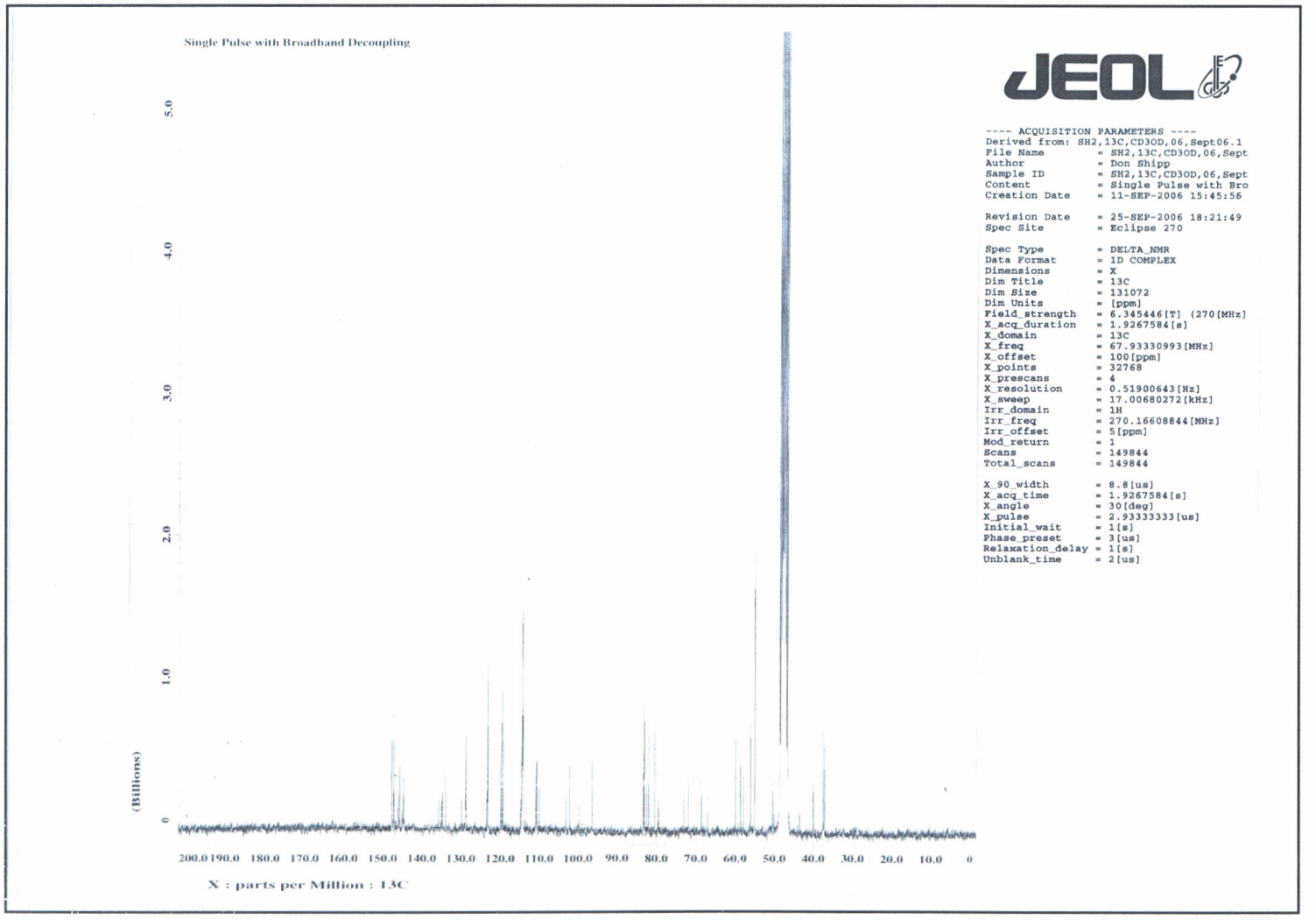

APPENDIX VIII (A): ASYMMETRIC UNIT OF ISOOLIVIL-ETHYL ACETATE

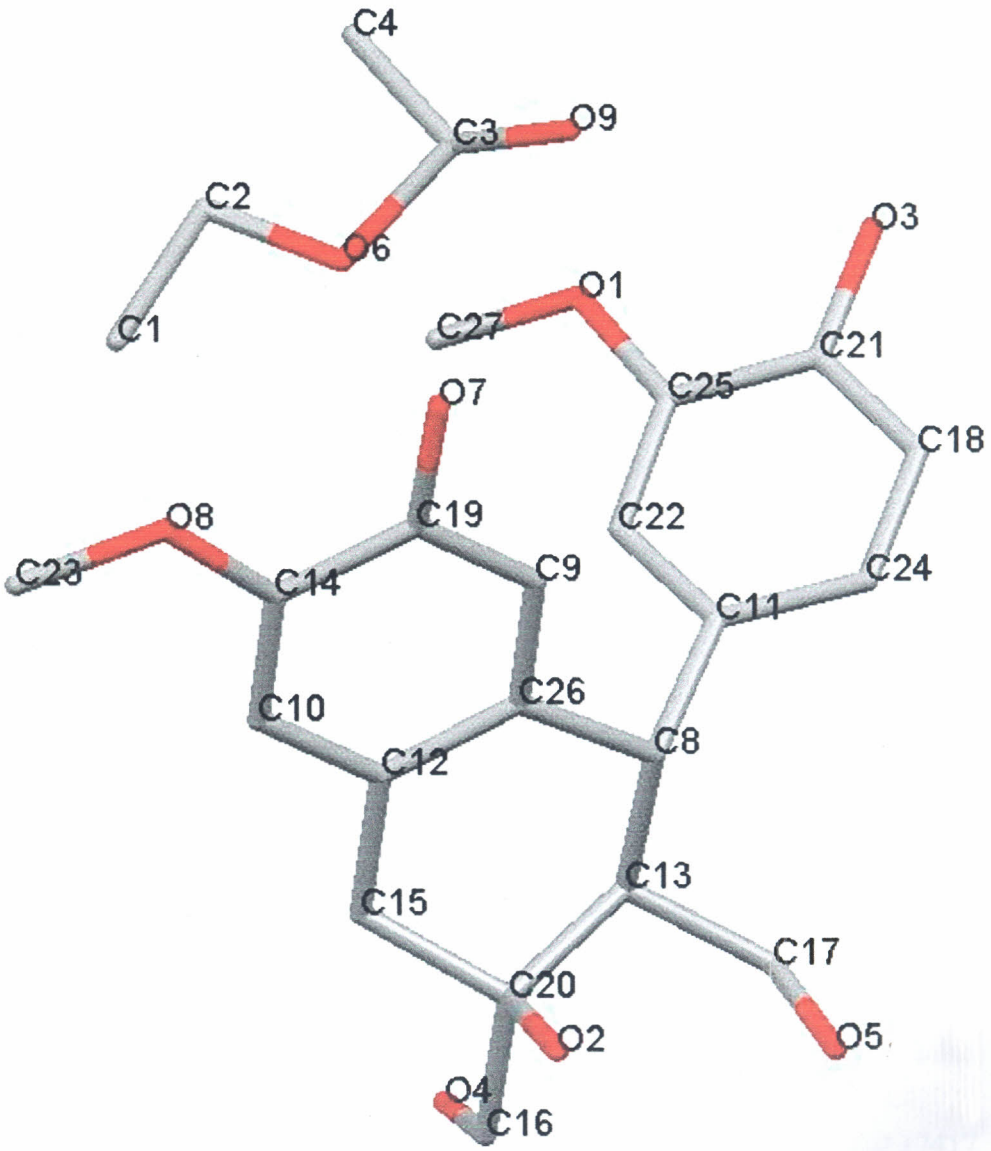

APPENDIX VIII (B): ATOMIC COORDINATES OF ISOOLIVI-ETHYL ACETATE SOLVATE

Atom	x	y	z
O1	0.68110	0.52098	0.16608
O2	0.63913	0.47000	0.53684
O3	1.03144	0.44748	0.13917
O4	0.22424	0.35605	0.46191
O5	0.83972	0.32973	0.49666
C8	0.78873	0.47990	0.40254
O7	0.95703	0.77288	0.37160
O8	0.60908	0.82573	0.41906
C9	0.86346	0.63157	0.38875
C10	0.50393	0.68103	0.44144
C11	0.84777	0.46458	0.33139
C12	0.55053	0.59582	0.43749
C13	0.62876	0.41684	0.42555
C14	0.63585	0.74072	0.41860
C15	0.40591	0.53184	0.46430
C16	0.36002	0.38653	0.50996
C17	0.72267	0.33087	0.43809
C18	1.08377	0.41969	0.25090
C19	0.82092	0.71615	0.39300
C20	0.50941	0.45053	0.48367
C21	0.96605	0.45248	0.20173
C22	0.72565	0.49376	0.28220
C23	0.41877	0.85569	0.43886
C24	1.02606	0.42685	0.31556
C25	0.78321	0.48883	0.21788
C26	0.73018	0.57116	0.41036
C27	0.48296	0.54173	0.17417
O6	0.66611	0.72021	0.23624
C1	0.38984	0.77040	0.26756
C3	0.82068	0.70979	0.18859
C4	0.70889	0.74655	0.13405
C2	0.51397	0.76575	0.21039
O9	1.00146	0.70012	0.19856

Bond lengths

O1-C25	1.3679 (29)
O1-C27	1.3795 (53)
O2-C20	1.4331 (28)
O3-C21	1.3637 (29)
O4-C16	1.4303 (32)
O5-C17	1.4396 (33)
C8-C26	1.5176 (33)
C8-C11	1.5379 (29)
C8-C13	1.5456 (32)
O7 - C19	1.3593 (33)
O8 - C14	1.3692 (30)
O8 - C23	1.4226 (38)
C9 - C19	1.3829 (36)
C9 - C26	1.3883 (35)
C10 - C14	1.3828 (37)
C10 - C12	1.3982 (35)
C11 - C24	1.3778 (38)
C11 - C22	1.3836 (34)
C12 - C26	1.3852 (34)
C12 - C15	1.5129 (34)
C13 - C17	1.5322 (33)
C13 - C20	1.5373 (31)
C14 - C19	1.4043 (38)
C15 - C20	1.5252 (34)
C16 - C20	1.5300 (35)
C18 - C21	1.3869 (37)
C18 - C24	1.3920 (35)
C21 - C25	1.3967 (37)
C22 - C25	1.3825 (33)
C1 - C2	1.4441 (115)
C3 - O9	1.2391 (200)
C3 - O6	1.4373 (110)
C3 - C4	1.4727 (128)
C2 - O6	1.3612 (113)

Bond angles

O1-C27-C25	118.55 (26)
C8-C11-C26	108.69 (18)
C8-C13-C11	111.56 (19)
O8 - C14-C23	116.93 (23)
C10 - C12-C14	120.52 (24)
C11 - C22-C24	119.17 (22)
C11 – C8-C24	121.23 (22)
C11 – C8-C22	119.48 (22)
C12 - C10-C26	119.63 (23)
C12 - C15-C26	120.85 (22)
C12 - C15-C10	119.50 (22)
C13 - C20-C17	113.34 (19)
C13 – C8-C17	110.49 (20)
C13 – C8-C20	111.86 (18)
C14 - C10-O8	126.66 (25)
C14 - C19-O8	113.29 (23)
C14 - C19-C10	120.04 (23)
C15 - C20-C12	112.24 (21)
C16 - C20-O4	113.51 (20)
C9 - C19-C26	121.69 (25)
C17 - C13-O4	112.12 (21)
C18 - C24-C21	120.65 (25)
C19 – C9-O7	119.45 (25)
C19 - C14-O7	121.94 (23)
C19 - C14-C9	118.61 (24)
C20 - C15-O2	106.95 (19)
C20 - C16-O2	105.76 (18)
C20 - C13-O2	110.81 (19)
C20 - C16-C15	111.30 (21)
C20 - C13-C15	109.33 (19)
C20 - C13-C15	112.52 (19)
C21 - C18-O3	119.03 (24)
C21 – C25-O3	122.12 (23)
C21 – C25-C18	118.85 (22)
C22 - C25-C11	121.18 (24)
C24 - C18-C11	120.24 (24)
C25 - C22-O1	125.93 (24)
C25 - C21-O1	114.17 (20)
C25 - C21-C22	119.81 (22)
C26 - C9-C12	119.45 (22)
C26 – C8-C12	122.73 (22)
C26 – C8-C9	117.81 (22)
O6 - C3-C2	109.57 (79)
C3 - O6-O9	127.35 (1.48)
C3 – C4-O9	132.38 (1.73)
C3 – C4-O6	96.20 (1.06)
C2 - C1-O6	98.06 (69)

APPENDIX IX (A): ASYMMETRIC UNIT OF ISOOLIVIL-HEMIHYDRATE

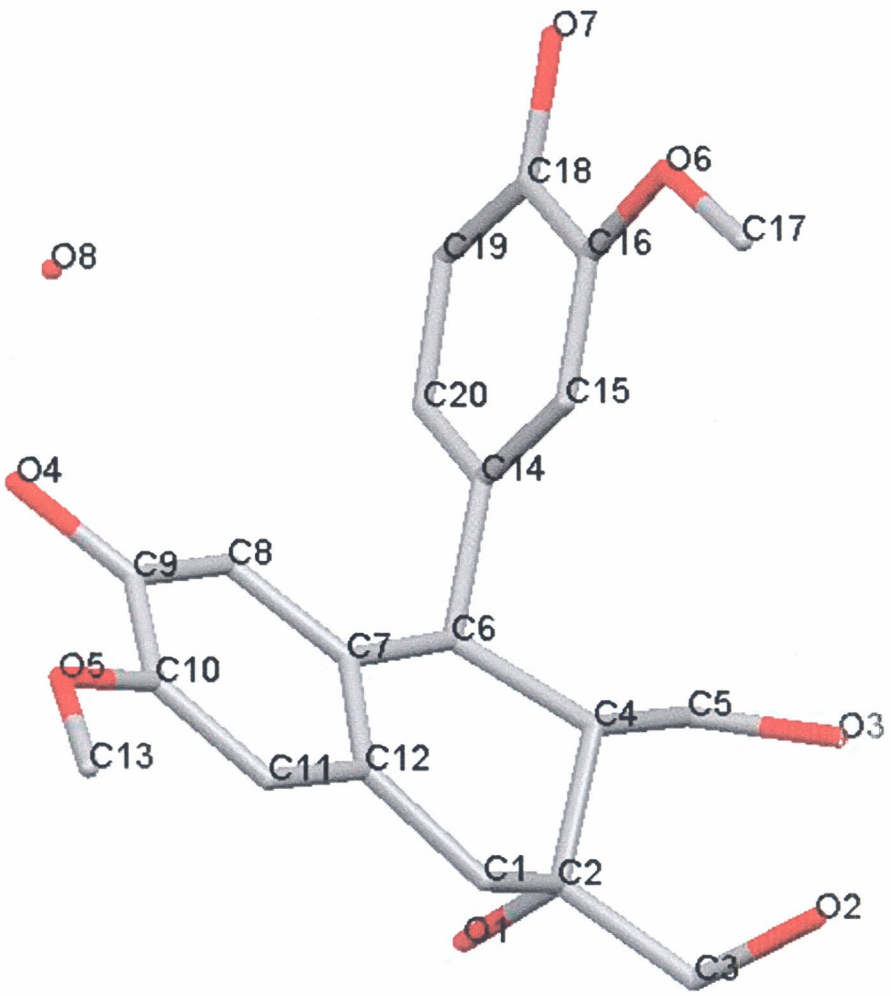

APPENDIX IX (B): ATOMIC COORDINATES OF ISOOLIVIL HEMIHYDRATE

ATOM	x	y	z
O1	0.67844	0.01626	0.09090
O7	0.53056	0.30969	0.87535
O3	0.67292	0.25742	0.08506
O6	0.71221	0.32062	0.76661
O5	0.92645	-0.12711	0.69509
O4	0.75017	-0.08762	0.83006
O2	0.84755	0.18895	0.00019
C9	0.77360	-0.05575	0.68307
C16	0.65337	0.26277	0.69587
C6	0.65611	0.09223	0.38847
C7	0.73052	0.03133	0.46226
C15	0.68457	0.21019	0.57667
C10	0.86433	-0.07786	0.60812
C8	0.70850	-0.00144	0.61209
C14	0.61852	0.15184	0.51388
C12	0.81676	0.00554	0.38311
C20	0.52123	0.14660	0.57388
C11	0.88350	-0.04880	0.45766
C18	0.55426	0.25632	0.75485
C2	0.75422	0.07517	0.13224
C5	0.62370	0.19065	0.16562
C4	0.70299	0.13693	0.24545
C17	0.80960	0.33513	0.69875
C3	0.79131	0.11485	-0.02222
C19	0.48857	0.19810	0.69530
C13	1.02567	-0.14181	0.63589
C1	0.84225	0.03430	0.21761
O8	0.50000	0.00000	0.90546

Bond lengths

O1 - C2	1.4320 (27)
O7 - C18	1.3773 (28)
O3 - C5	1.4415 (28)
O6 - C16	1.3621 (29)
O6 - C17	1.4274 (30)
O5 - C10	1.3643 (28)
O5 - C13	1.4223 (32)
O4 - C9	1.3823 (29)
O2 - - C3	1.4337 (28)
C9 - C10	1.4020 (34)
C16 - C18	1.4038 (34)
C6 - C14	1.5232 (30)
C6 - C7	1.5314 (30)
C7 - C12	1.3859 (32)
C7 - C8	1.4055 (31)
C15 - C16	1.3871 (33)
C10 - C11	1.3809 (33)
C8 - C9	1.3736 (32)
C14 - C20	1.3831 (33)
C14 - C15	1.3972 (33)
C11 - C12	1.4010 (32)
C18 - C19	1.3826 (33)
C2 - C3	1.5379 (32)
C2-C4	1.5469 (30)
C4 - C5	1.5239 (32)
C4 - C6	1.5422 (31)
C19 - C20	1.3958 (34)
C1 - C12	1.5137 (30)
C1 - C2	1.5222 (32)

Bond Angles

O6 - C17-C16	116.90 (0.18)
O5 - C13-C10	117.62 (0.20)
C9 - O4-C8	119.76 (0.22)
C9 – C10-C8	120.24 (0.22)
C9 – C10-O4	119.99 (0.21)
C16 - C15-O6	125.47 (0.22)
C16 - C18-O6	115.31 (0.21)
C16 - C18-C15	119.20 (0.22)
C6 - C7-C14	109.99 (0.19)
C6 – C4-C14	111.88 (0.18)
C6 – C4-C7	111.73 (0.18)
C7 - C8-C12	119.25 (0.21)
C7 – C6-C12	121.87 (0.20)
C7 – C6-C8	118.84 (0.20)
C15 - C14-C16	120.94 (0.22)
C10 - C11-O	126.09 (0.22)
C10 – C9-O5	114.97 (0.22)
C10 – C9-C11	118.93 (0.22)
C8 - C7-C9	120.71 (0.22)
C14 - C15-C20	118.83 (0.21)
C14 – C6-C20	121.19 (0.21)
C14 – C6-C15	119.88 (0.21)
C12 - C11-C7	119.50 (0.21)
C12 - C1-C7	122.27 (0.20)
C12 - C1-C11	118.23 (0.20)
C20 - C19-C14	121.25 (0.22)
C11 - C12-C10	121.14 (0.22)
C18 - C19-O7	124.28 (0.22)
C18 - C16-O7	115.25 (0.22)
C18 - C16-O7	120.45 (0.22)
C2 - C1-O1	110.69 (0.19)
C2 – C3-O1	107.40 (0.18)
C2 – C4-O1	106.56 (0.18)
C2 – C3-C1	110.16 (0.19)
C2 – C4-C1	109.10 (018)
C2 – C4-C3	112.87 (0.18)
C5 - C4-O3	109.66 (0.19)
C4 - C6-C5	110.17 (0.19)
C4 – C2-C5	113.75 (0.19)
C4 – C2-C6	110.53 (0.18)
C3 - C2-O2	114.17 (0.19)
C19 - C20-C18	119.31 (0.22)
C1 - C2-C12	113.88 (0.19)

APPENDIX X (A): ASYMMETRIC UNIT OF ISOOLIVIL-WATER-ACETONITRILE SOLVATE

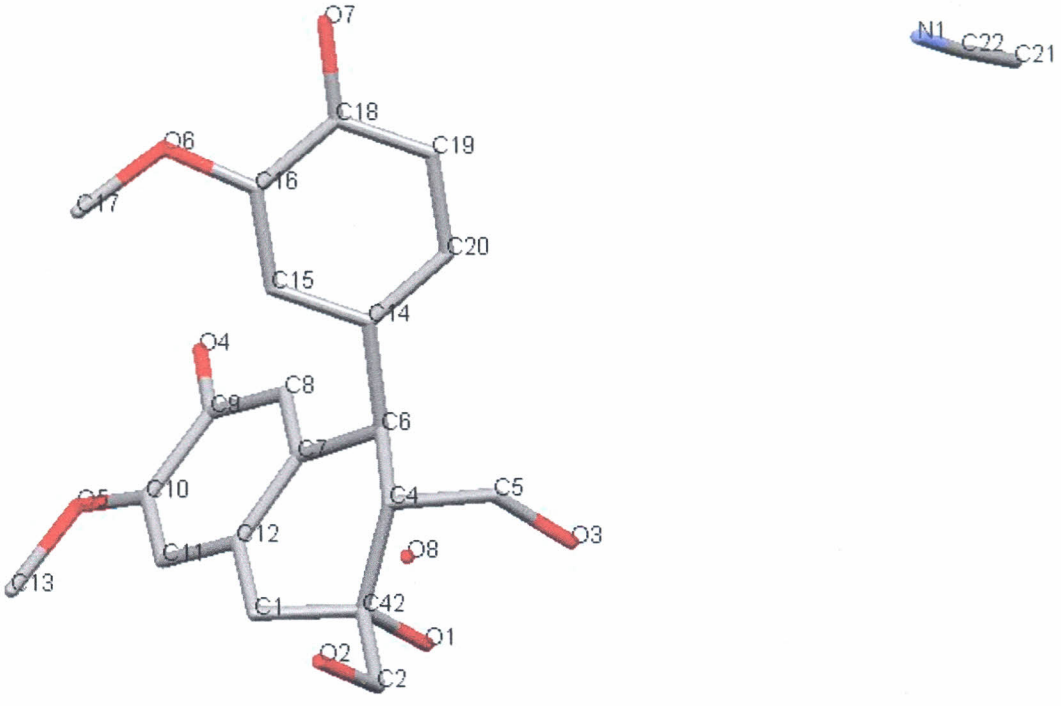

APPENDIX X (B): ATOMIC COORDINATES FOR ISOOLIVIL-WATER-ACETONITRILE SOLVATE

ATOM	x	y	z
O7	0.96376	0.94138	0.13942
O1	1.36004	0.99544	0.53412
O3	1.16143	0.86198	0.50038
O2	1.78673	0.88695	0.46381
O6	1.31480	1.01935	0.16192
O4	1.03747	1.27524	0.36501
C6	1.20822	0.99803	0.40016
C8	1.13166	1.14126	0.38328
C14	1.14559	0.97912	0.33078
O5	1.38918	1.32553	0.41105
C7	1.26963	1.08470	0.40564
C4	1.37206	0.93957	0.42492
C15	1.26858	1.00488	0.27914
O8	1.71126	0.75011	0.40311
C5	1.27634	0.85929	0.44076
C12	1.45199	1.10909	0.43270
C10	1.36334	1.24563	0.41158
C11	1.49778	1.19005	0.43570
C2	1.64461	0.91525	0.51093
C1	1.59886	1.04944	0.46045
C13	1.57276	1.35579	0.43777
C42	1.49279	0.97446	0.48176
C9	1.17641	1.22159	0.38637
C18	1.02844	0.95440	0.20130
C20	0.96734	0.94017	0.31623
C16	1.20945	0.99343	0.21521
C19	0.90917	0.92712	0.25193
C17	1.48781	1.06718	0.17374
N1	0.94416	0.21237	0.17897
C22	0.82468	0.23720	0.21337
C21	0.66795	0.27128	0.25213

Bond lengths

O7 - C18	1.3608 (25)
O1 - C42	1.4334 (24)
O3 - C5	1.4432 (28)
O2 - C2	1.4316 (27)
O6 - C16	1.3703 (24)
O6 - C17	1.4206 (31)
O4 - C9	1.3629 (28)
C6 - C14	1.5201 (26)
C6 - C7	1.5248 (27)
C8 - C9	1.3916 (31)
C14 - C20	1.3815 (31)
C14 - C15	1.4063 (27)
C14 - C6	1.5201 (26)
O5 - C10	1.3618 (27)
O5 - C13	1.4260 (29))
C7 - C12	1.3893 (29)
C7 - C8	1.3986 (31)
C4 - C42	1.5332 (28)
C4 - C5	1.5324 (30)
C4 - C6	1.5514 (26)
C15 - C16	1.3857 (27)
C10 - C11	1.3847 (32)
C11 - C12	1.4032 (30)
C2 - C42	1.5386 (28)
C1 - C12	1.5112 (29)
C1 - C42	1.5134 (30)
C9 - C10	1.3992 (31)
C18 - C19	1.3849 (30)
C16 - C18	1.3950 (32)
C19 - C20	1.3951 (30)
N1 - C22	1.1400 (65)
C21 - C22	1.4279 (68)

Bond angles

O6 - C17-C16	116.97 (17)
C6 - C7-C14	110.11 (16)
C6 – C4-C14	111.35 (16)
C6 – C4-C7	113.74 (16)
C8 - C7-C9	120.94 (20)
C14 - C15-C20	118.42 (18)
C14 - C6-C20	122.37 (19)
C14 - C6-C15	119.15 (18)
O5 - C13-C10	117.35 (20))
C7 – C8-C12	119.56 (20)
C7 – C6-C12	123.06 (19)
C7 – C6-C8	117.37 (18)
C4 - C5-C42	113.14 (17)
C4 – C6-C42	111.58 (16)
C4 – C6-C5	110.28 (16)
C15 - C14-C16	120.74 (19)
C5 - C4-O3	111.70 (18)
C12 - C11-C7	119.60 (19)
C12 - C1-C7	120.63 (20)
C12 - C1-C11	119.75 (19)
C10 - C11-O5	126.57 (21)
C10 - C9-O5	113.31 (20)
C10 - C9-C11	120.09 (20)
C11 - C12-C10	120.54 (19)
C2 - C42-O2	112.36 (16)
C1 - C42-C12	111.82 (17)
C42 - C1-O1	107.05 (17)
C42 – C4-O1	110.52 (16)
C42 – C2-O1	105.45 (15)
C42 – C4-C1	110.00 (16)
C42 – C2-C1	110.89 (17)
C42 – C2-C4	112.70 (17)
C9 - C8-O4	119.47 (20)
C9 – C10-O4	121.34 (21)
C9 – C10-O8	119.19 (20)
C18 - C19-O7	118.12 (20)
C18 - C16-O7	122.50 (20)
C18 - C16-C19	119.38 (19)
C20 - C19-C14	121.03 (20)
C16 - C15-O6	124.87 (19)
C16 - C18-O6	114.98 (17)
C16 - C18-C15	120.14 (19)
C19 - C20- C18	120.26 (20)
C22 - C21-N1	175.49 (60)

APPENDIX X (A): ASYMMETRIC UNIT OF EPIFRIEDELINOL

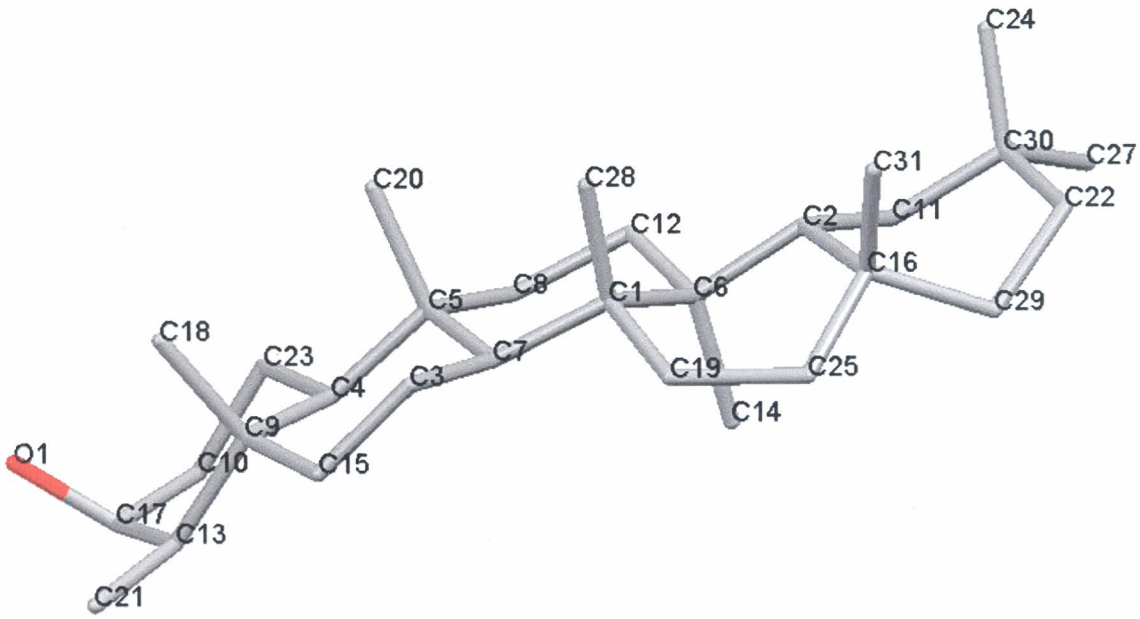

APPENDIX XI (B): ATOMIC COORDINATES FOR EPIFRIEDELINOL

Atom	x	y	z
C1	0.29780	0.32930	0.26231
C2	0.23684	0.26806	0.34245
C3	0.35408	0.40631	0.18049
C4	0.14591	0.49384	0.15083
C5	0.16699	0.35213	0.19340
C6	0.21162	0.38303	0.29726
C7	0.27149	0.41833	0.21516
C8	0.08699	0.38539	0.22709
C9	0.23141	0.51118	0.11476
C10	0.02048	0.65549	0.09599
C11	0.15743	0.31861	0.37833
C12	0.11158	0.29397	0.27503
C13	0.20418	0.69748	0.08233
C14	0.19416	0.62836	0.30431
C15	0.33312	0.55199	0.14121
C16	0.34660	0.32329	0.36273
C17	0.10382	0.68798	0.06178
C18	0.24233	0.30588	0.08774
19	0.39511	0.44161	0.28044
C20	0.16145	0.11571	0.17852
C21	0.28484	0.75601	0.04704
C22	0.28385	0.27652	0.44313
C23	0.04496	0.46606	0.12699
C25	0.40542	0.46863	0.33487
O1	0.09506	0.55212	0.02582
C27	0.09341	0.27962	0.45575
C28	0.31969	0.10472	0.25958
C29	0.33876	0.43643	0.41203
C30	0.17300	0.20335	0.42468
C31	0.41122	0.11461	0.37110
C24	0.16640	-0.00780	0.42320

Bond lengths

C1 -C28	1.5206 (137)
C1 -C7	1.5569 (117)
C1 -C19	1.6057 (123)
C1 -C6	1.5976 (107)
C2 - C6	1.5673 (106)
C2 -C11	1.5763 (137)
C2 -C16	1.6408 (136)
C3 -C15	1.5378 (115)
C3 -C7	1.5641 (113)
C4 -C23	1.5398 (115)
C4 -C5	1.5680 (109)
C4 -C9	1.5979 (105)
C5 -C8	1.5444 (116)
C5 -C20	1.5805 (117)
C5 -C7	1.5597 (115)
C6 -C12	1.5562 (110)
C6 -C14	1.6230 (132)
C8 -C12	1.5851 (119)
C9 -C18	1.5582 (122)
C9 -C13	1.5897 (113)
C9 -C15	1.5652 (114)
C10 -C23	1.5409 (133)
C10 -C17	1.5741 (136)
C11 -C30	1.5492 (173)
C13 -C17	1.4957 (128)
C13 -C21	1.5548 (123)
C16 -C25	1.5460 (154)
C16 -C31	1.6025 (176)
C16 -C29	1.5977 (162)
C19 -C25	1.6061 (133)
C22 -C29	1.5668 (196)
C22 -C30	1.6343 (196)
O1 - C17	1.3883 (136)
C27 - C30	1.5767 (197)
C24 - C30	1.4539 (208)

Bond angles

C1 -C7-C28	110.42 (73)
C1 –C19-C28	106.11 (71)
C1 –C6-C28	113.91 (68)
C1 –C19-C7	108.10 (69)
C1 –C6-C7	110.71 (64)
C1 –C6-C19	107.28 (65)
C2 -C11-C6	111.67 (70)
C2 –C16-C6	114.02 (68)
C2 -C16-C11	109.60 (75)
C3 -C7-C15	110.62 (66)
C4 -C5-C23	115.59 (67)
C4 –C9-C23	110.47 (63)
C4 –C9-C5	116.83 (64)
C5 -C4-C8	109.97 (64)
C5 –C20-C8	105.90 (65)
C5 –C7-C8	108.93 (64)
C5 –C20-C4	109.97 (64)
C5 –C7-C4	107.78 (63)
C5 –C7-C20	114.58 (66)
C6 -C12-C2	108.76 (61)
C6 –C14-C2	110.76 (65)
C6 –C1-C2	108.52 (59)
C6 –C14-C12	108.25 (67)
C6 -C1-C12	107.03 (61)
C6 -C1-C14	113.37 (65)
C7 -C3-C1	115.34 (66)
C7 –C5-C1	116.82 (68)
C7 –C5-C3	111.35 (65)
C8 -C12-C5	114.39 (67)
C9 -C13-C18	109.80 (62)
C9 -C15-C18	108.27 (66)
C9 –C4-C18	113.06 (65)
C9 -C15-C13	109.09 (65)
C9 –C4-C13	107.79 (62)
C9 –C4-C15	108.77 (61)
C10 -C17C23	111.67 (78)
C11 -C2-C30	115.90 (94)
C12 -C6-C8	112.02 (67)
C13 -C9-C17	114.11 (71)
C13 –C21-C17	111.71 (72)
C13 –C21-C9	116.92 (67)
C15 -C9-C3	113.48 (68)
C16 -C31-C25	109.07 (87)
C16 –C2-C25	113.31 (81)
C16 –C29-C25	106.40 (94)
C16 –C2-C31	110.01 (90)
C16 –C29-C31	109.77 (91)
C16 –C29-C2	108.18 (83)
C17 -C13-O1	112.93 (84)
C17 -C10-O1	112.29 (87)
C17 -C10-C13	113.40 (77)
C19 -C25-C1	116.14 (72)
C22 -C30-C29	110.45 (1.10)
C23 -C10-C4	110.20 (73)
C25 - C19-C16	116.91 (82)
C29 -C16-C22	110.10 (1.11)
C30 -C27-C24	105.84 (1.22)
C30 –C11-C24	113.64 (1.19)
C30 –C22-C24	111.04 (1.22)
C30 –C11-C27	108.15 (1.12)
C30 –C22-C27	109.37 (1.13)
C30 -C22-C11	108.67 (1.06)

APPENDIX XII (A): ASYMMETRIC UNIT OF HENNINGNOL

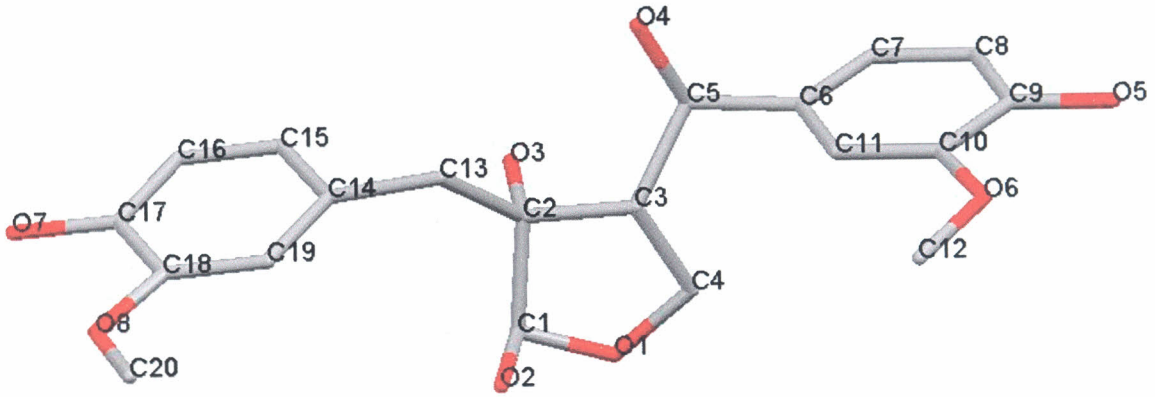

APPENDIX XII (B): ATOMIC COORDINATES FOR HENNINGNOL

Atom	x	y	z
C6	0.54823	1.10700	1.18626
O1	0.04482	0.90230	1.00652
O2	-0.13381	1.07528	0.92780
O4	0.65897	1.20766	1.05928
O3	0.45308	0.96208	0.92683
C4	0.17537	0.96583	1.07870
C3	0.29923	1.08294	1.04372
C2	0.27816	1.05312	0.94561
C11	0.39683	1.19053	1.22433
O7	0.13487	1.12545	0.52414
C5	0.54357	1.09668	1.08971
C10	0.40859	1.19980	1.31263
C1	0.04519	0.98198	0.93309
C14	0.24590	1.15125	0.79212
C17	0.17046	1.13262	0.61291
C13	0.29382	1.17331	0.88833
C19	0.05655	1.21026	0.74555
C8	0.72149	1.04726	1.32856
O5	0.58422	1.13559	1.45262
C16	0.35744	1.07044	0.65736
C18	0.01902	1.20276	0.65786
O6	0.26778	1.27370	1.35740
C9	0.57110	1.12818	1.36578
C15	0.39489	1.08172	0.74577
C20	-0.30329	1.34694	0.64221
C7	0.70775	1.03731	1.23988
O8	-0.15723	1.25898	0.60555
C12	0.08168	1.34092	1.30847

Bond lengths

O4 - C5	1.4268 (36)
O2 - C1	1.4084 (32)
O1 - C1	1.4044 (38)
O1 - C4	1.4376 (39)
C6 - C7	1.3745 (51)
C6 - C11	1.4072 (48)
C3 -C5	1.5249 (40)
C3 -C4	1.5297 (41)
C2 -O3	1.4350 (31)
C2 -C13	1.5267 (40)
C2 -C3	1.5499 (41)
O7 - C17	1.3768 (45)
C5 -O4	1.4268 (36)
C5 -C6	1.5056 (43)
C10 -C11	1.3730 (50)
C1 -C2	1.5326 (36)
C14 -C15	1.3878 (49)
C14 -C19	1.3865 (47)
C17 - C18	1.3882 (60)
C13 -C14	1.5101 (46)
C8 -C9	1.3807 (71)
O5 - C9	1.3488 (46)
C16 -C17	1.3769 (61)
C18- C19	1.3608 (53)
O6 -C10	1.3650 (52)
O6 -C12	1.4275 (79)
C9 -C10	1.3916 (64)
C15 -C16	1.3747 (54)
C7 -C8	1.3788 (58)
O8 - C18	1.3621 (51)
O8 -C20	1.4040 (70)

Bond angles

O1 - C4-C1	108.99 (22)
C6 - C11-C7	118.08 (33)
C6 – C5-C7	120.25 (31)
C6 – C5-C11	121.63 (30)
C4 - C3-O1	107.63 (25)
C3 –C4-C5	111.00 (25)
C3 –C2-C5	116.39 (22)
C3 –C2-C4	102.20 (23)
C2-C13-O3	108.03 (22)
C2-C1-O3	107.88 (21)
C2-C3-O3	110.59 (22)
C2-C1-C13	114.77 (24)
C2-C3-C13	114.56 (24)
C2-C3-C1	100.74 (21)
C11 -C6-C10	120.24 (36)
C5-C6-O4	108.79 (25)
C5-C3-O3	111.57 (25)
C5-C3-O6	112.56 (24)
C10 –C11-O6	125.97 (41)
C10 –C9-O6	113.23 (36)
C10 –C9-C11	120.78 (37)
C1 -O2-O1	111.62 (22)
C1 -C2-O1	104.84 (23)
C1 -C2-O2	109.04 (22)
C14 -C19-C15	117.28 (33)
C14 –C13-C15	122.57 (30)
C14 -C13-C19	119.95 (29)
C17 - O7-C16	119.95 (38)
C17 – C18-C16	119.78 (35)
C17 – C18-O7	120.27 (37)
C13 -C2-C14	116.36 (25)
C19 -C14-C18	121.78 (35)
C8 -C7-C9	119.97 (40)
C16 -C17-C15	119.34 (38)
C18-O8-C19	126.83 (41)
C18-C17-C19	119.89 (35)
C18-C17-O8	113.28 (38)
O6 -C12-C10	117.24 (35)
C9 -C8-O5	119.37 (44)
C9 –C10-O5	121.55 (44)
C9 –C10-C8	119.08 (34)
C15 -C14-C16	121.90 (36)
C7 -C8-C6	121.85 (41)
O8 -C20-C18	118.49 (38)

APPENDIX XIII (A): ASYMMETRIC UNIT OF ß-SITOSTEROL

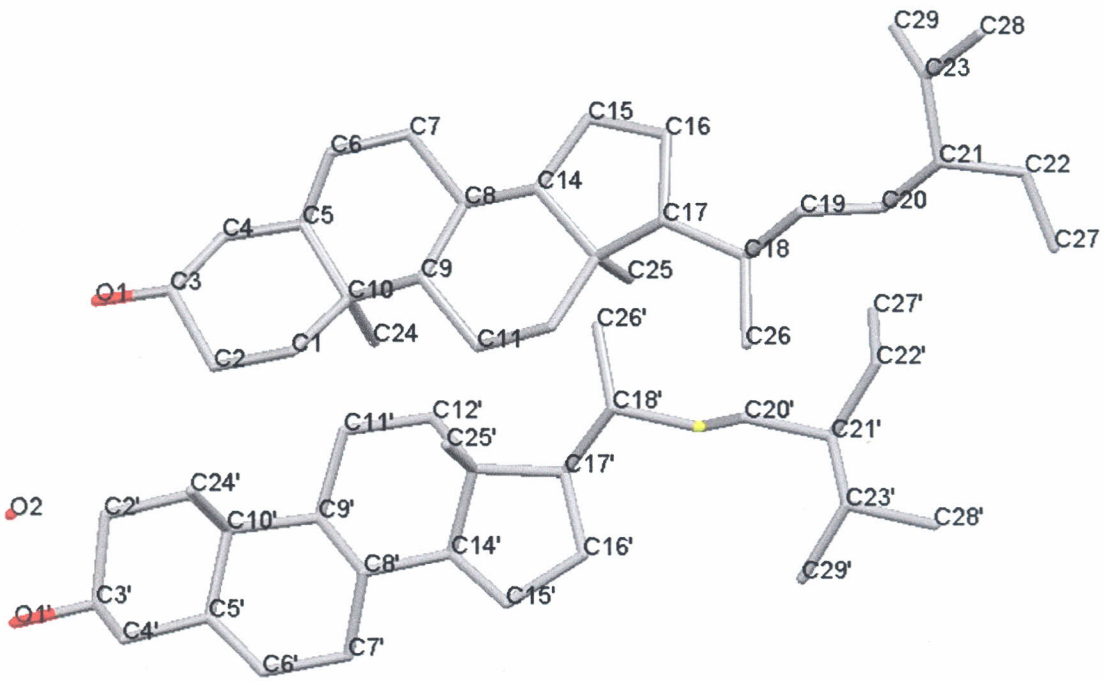

Atom	x	y	z
C10'	0.36502	0.83493	0.04831
O1	-0.28142	1.32071	0.01690
C8	-0.33606	1.30283	0.10577
C8'	0.52711	0.79039	0.07869
11'	0.19262	0.84437	0.07873
10	-0.17689	1.32094	0.07498
C9	-0.18083	1.24830	0.09409
C9'	0.37371	0.86785	0.06904
14'	0.51893	0.82235	0.09892
C7'	0.70294	0.83766	0.07077
C13'	0.34498	0.77932	0.10831
C11	-0.00223	1.25837	0.10408
O1'	0.46078	0.97074	-0.00736
C5'	0.55373	0.84006	0.04033
C7	-0.51323	1.27098	0.09663
C13	-0.15265	1.26264	0.13493
C14	-0.32796	1.23663	0.12463
C1	-0.06832	1.22697	0.06182
C12	-0.00590	1.19369	0.12322
C17	-0.19379	1.18965	0.15336
C5	-0.36517	1.33339	0.06729
C6'	0.70050	0.84262	0.05049
C3	-0.26632	1.27777	0.03543
C4'	0.56515	0.84663	0.01970
C2	-0.07547	1.27751	0.04220
C6	-0.51094	1.30786	0.07698
C25'	0.30484	0.61926	0.10657
C3'	0.45383	0.96826	0.01221
C4	-0.37798	1.37387	0.04750
C15'	0.66496	0.75932	0.11100
C1'	0.25265	0.94916	0.03879

Atom	x	y	z
C24'	0.28568	0.68608	0.04456
C2'	0.26126	0.94975	0.01823
C25	-0.11435	1.42304	0.13793
C18'	0.27368	0.74922	0.14347
C19'	0.34920	0.78372	0.16194
C24	-0.09204	1.47023	0.07582
C16'	0.58706	0.77384	0.13036
C16	-0.39298	1.22731	0.15674
C15	-0.47070	1.27559	0.13829
C26	0.11762	1.19996	0.16734
C26'	0.07632	0.78998	0.14246
C18	-0.08317	1.22662	0.17000
C19	-0.14595	1.13958	0.18641
C21	-0.19543	1.12862	0.22076
C20'	0.36348	0.67995	0.17509
C22'	0.30142	0.66087	0.20814
C23'	0.61482	0.61722	0.19645
C21'	0.44047	0.70772	0.19379
C20	-0.13033	1.21021	0.20402
O2	0.30502	0.39352	0.00854
C29'	0.75451	0.65728	0.18241
C22	-0.14900	1.21773	0.23813
C28'	0.69447	0.64205	0.21544
C28	-0.45054	1.01737	0.23777
C23	-0.39311	1.10389	0.22151
C27'	0.16810	0.76673	0.20717
C29	-0.52700	1.18962	0.21447
C27	0.02915	1.24466	0.24124

Bond lengths

C10' -C24'	1.5421 (47)
O1 - C3	1.4293 (42)
C8-C14	1.5246 (44)
C8-C9	1.5373 (44)
C8' -C14'	1.5232 (45)
C8' -C9'	1.5369 (43)
C11' -C12'	1.5316 (47)
C10 -C24	1.5389 (46)
C9 -C11	1.5333 (45)
C9 -C10	1.5659 (42)
C9 -C11	1.5524 (45)
C9 -C8	1.5369 (43)
C9 -C10	1.5610 (46)
C14' -C15'	1.5321 (45)
C7' -C8'	1.5106 (46)
C13' -C25'	1.5356 (49)
C13' -C14'	1.5331 (44)
C11 -C9	1.5333 (45)
C11 -C12	1.5372 (45)
O1' - C3'	1.4446 (43)
C5' -C6'	1.3329 (52)
C5' -C10'	1.5356 (47)
C6	1.4900 (48)
C7 -C8	1.5215 (46)
C13 -C14	1.5395 (48)
C13 -C25	1.5466 (52)
C13 -C17	1.5534 (46)
C14 -C15	1.5157 (47)
C1 -C2	1.5239 (46)
C1 -C10	1.5438 (43)
C12 -C13	1.5422 (48)
C17 -C18	1.5221 (55)
C5 -C6	1.3296 (50)
C5 -C10	1.5283 (47)
C6' - C7'	1.4970 (49)
C3 -C4	1.5189 (54)
C12' -C13'	1.5387 (46)
C4' -C5'	1.5257 (50)
C2 -C3	1.5180 (52)
C17' -C18'	1.5333 (52)
C6 -C7	1.4900 (48)
C3' -C4'	1.5180 (58)
C4 -C5	1.5115 (50)
C15' -C16'	1.5489 (53)
C1' -C2'	1.5180 (47)
C1' -C10'	1.5336 (48)
C2' -C3'	1.5231 (52)
C18' -C19'	1.5103 (55)
C18' -C26'	1.5328 (56)
C19' -C20'	1.3778 (76)
C16' -C17'	1.5576 (51)
C16 -C17	1.5574 (56)
C15 -C16	1.5487 (57)
C18 -C19	1.5335 (62)
C18 -C26	1.5414 (65)
C19 -C20	1.4633 (73)
C21 -C23	1.5039 (0143)
C21 -C22	1.5687 (0143)
C20'-C21'	1.5183 (79)
C22' -C27'	1.4116 (0337)
C23' -C29'	1.5215 (0115)
C23' -C28'	1.5408 (0102)
C21' -C22'	1.5509 (0136)
C21' -C23'	1.5728 (0105)
C20 -C21	1.5325 (92)
C22 -C27	1.3809 (0180)
C23 -C29	1.3882 (0174)
C23 -C28	1.5109 (0120)

Bond angles

C10' -C1'-C5'	108.11 (28)
C10' –C24'-C5'	108.45 (29)
C10' –C9'-C5'	109.29 (27)
C10' –C24'-C1'	109.68 (29)
C10' –C9'-C1'	109.48 (28)
C10' –C9'-C24'	111.76 (28)
C8-C14-C7	111.06 (28)
C8-C9-C7	110.49 (26)
C8-C9-C14	110.23 (26)
C8' -C14'- C7' -	110.88 (27)
C8' –C9'- C7' -	109.75 (26)
C8' –C9'- C14' -	109.30 (26)
C10 -C24-C5	109.20 (29)
C10 –C1-C5	107.41 (26)

C10 –C9-C5	110.48 (27)	C13 –C17-C12	116.60 (30)	C1' -C10' -C2'	115.88 (30)
C10 –C1-C24	108.99 (27)	C13 -C17-C25	109.87 (29)	C2' -C3' -C1'	109.40 (30)
C10 –C9-C24	111.52 (26)	C14 -C8-C15	118.69 (30)	C18' -C17' -C19'	110.89 (35)
C10 –C9-C1	109.14 (26)	C14 –C13-C15	103.85 (27)	C18' –C26' -C19'	110.72 (34)
C9 -C8-C11	111.96 (26)	C14 –C13-C8	114.82 (28)	C18' –C26' –C17'	113.70 (32)
C9 –C10-C11	112.90 (26)	C1 -C10-C2	113.65 (28)	C19' -C18' -C20'	120.85 (49)
C9 –C10-C8	111.98 (26)	C12 -C13-C11	111.22 (28)	C16' -C17'- C15'	107.55 (28)
C9 –C11-C8	112.14 (26)	C17 -C13-C18	119.80 (35)	C16 -C17-C15	106.73 (30)
C9 –C10-C8	113.05 (27)	C17 -C16-C18	110.12 (31)	C15 -C16-C14	104.30 (31)
C9 –C10-C11	112.72 (26)	C17 -C16-C13	103.38 (30)	C19 -C18-C20	115.81 (54)
C14' -C15'-C8'	117.73 (27)	C5 -C4-C6	120.82 (33)	C21 -C20-C23	108.74 (86)
C14' -C13'-C8'	115.18 (26)	C5 –C10-C6	120.82 (33)	C21 -C22-C23	105.77 (93)
C14' -C13'-C15'	104.23 (26)	C5 –C10-C4	120.82 (33)	C21 -C22-C20	108.74 (86)
C7' -C8'-C6'	112.63 (29)	C6' - C7' C5'	124.82 (32)	C20'-C21' -C19'	123.24 (66)
C13' -C14'-C25'	112.74 (28)	C3 -C2-O1	112.95 (30)	C22' -C21' -C27'	104.13 (1.62)
C13' -C12'-C25'	110.71 (29)	C3 –C4-O1	110.45 (32)	C23' -C28' -C29'	108.29 (79)
C13' -C17'-C25'	109.55 (28)	C3 –C4-C2	109.25 (29)	C23' -C21' -C29'	110.86 (59)
C13' -C12'-C14'	105.85 (26)	C12' -C13'- C11'	111.54 (27)	C23' -C21' -C28'	110.82 (68)
C13' -C17'-C24'	101.48 (26)	C4' -C5' -C3'	111.25 (31)	C21' -C22' -C20'	108.38 (74)
C13' -C17'-C12'	116.21 (27)	C2 -C1-C3	110.25 (29)	C21' -C23' -C20'	109.77 (60)
C11 -C12-C9	113.66 (28)	C17' -C13' -C18'	119.16 (31)	C21' -C23' -C22'	108.83 (75)
C5' -C4'-C6'	120.88 (33)	C17' -C16' -C18'	111.54 (30)	C20 -C21-C19	117.66 (71)
C5' –C10'-C6'	123.30 (32)	C17' -C16' -C13'	103.24 (28)	C22 -C21-C27	116.63 (1.34)
C5' –C10'-C4'	115.80 (30)	C6 -C7-C5	125.06 (32)	C23 -C28-C29	113.63 (1.17)
C7 -C8-C6	112.04 (28)	C3' -C4' -O1'	110.85 (32)	C23 -C28-C29	127.77 (1.21)
C13 -C12-C14	105.61 (26)	C3' –C2' -O1'	109.11 (31)	C23 -C28-C29	113.19 (98)
C13 –C25-C14	112.56 (29)	C3' –C2' –C4'	109.36 (33)	C10' -C1'-C5'	108.11 (28)
C13 -C17-C14	101.06 (28)	C4 -C3-C5	112.46 (31)	C10' –C24'-C5'	108.45 (29)
C13 –C25-C12	110.76 (31)	C15' -C16' -C14'	103.41 (28)	C10' –C9'-C5'	109.29 (27)

C10' –C24'-C1'	109.68 (29)	C13' -C17'-C24'	101.48 (26)	C4' -C5' -C3'	111.25 (31)
C10' –C9'-C1'	109.48 (28)	C13' -C17'-C12'	116.21 (27)	C2 -C1-C3	110.25 (29)
C10' –C9'-C24'	111.76 (28)	C11 -C12-C9	113.66 (28)	C17' -C13' -C18'	119.16 (31)
C8-C14-C7	111.06 (28)	C5' -C4'-C6'	120.88 (33)	C17' -C16' -C18'	111.54 (30)
C8-C9-C7	110.49 (26)	C5' –C10'-C6'	123.30 (32)	C17' -C16' -C13'	103.24 (28)
C8-C9-C14	110.23 (26)	C5' –C10'-C4'	115.80 (30)	C6 -C7-C5	125.06 (32)
C8' -C14'- C7' -	110.88 (27)	C7 -C8-C6	112.04 (28)	C3' -C4' -O1'	110.85 (32)
C8' –C9'- C7' -	109.75 (26)	C13 -C12-C14	105.61 (26)	C3' –C2' -O1'	109.11 (31)
C8' –C9'- C14' -	109.30 (26)	C13 –C25-C14	112.56 (29)	C3' –C2' –C4'	109.36 (33)
C10 -C24-C5	109.20 (29)	C13 -C17-C14	101.06 (28)	C4 -C3-C5	112.46 (31)
C10 –C1-C5	107.41 (26)	C13 –C25-C12	110.76 (31)	C15' -C16' -C14'	103.41 (28)
C10 –C9-C5	110.48 (27)	C13 –C17-C12	116.60 (30)	C1' -C10' -C2'	115.88 (30)
C10 –C1-C24	108.99 (27)	C13 -C17-C25	109.87 (29)	C2' -C3' -C1'	109.40 (30)
C10 –C9-C24	111.52 (26)	C14 -C8-C15	118.69 (30)	C18' -C17' -C19'	110.89 (35)
C10 –C9-C1	109.14 (26)	C14 –C13-C15	103.85 (27)	C18' –C26' -C19'	110.72 (34)
C9 -C8-C11	111.96 (26)	C14 –C13-C8	114.82 (28)	C18' –C26' –C17'	113.70 (32)
C9 –C10-C11	112.90 (26)	C1 -C10-C2	113.65 (28)	C19' -C18' -C20'	120.85 (49)
C9 –C10-C8	111.98 (26)	C12 -C13-C11	111.22 (28)	C16' -C17'- C15'	107.55 (28)
C9 –C11-C8	112.14 (26)	C17 -C13-C18	119.80 (35)	C16 -C17-C15	106.73 (30)
C9 –C10-C8	113.05 (27)	C17 -C16-C18	110.12 (31)	C15 -C16-C14	104.30 (31)
C9 –C10-C11	112.72 (26)	C17 -C16-C13	103.38 (30)	C18 -C19-C17	110.31 (40)
C14' -C15'-C8'	117.73 (27)	C5 -C4-C6	120.82 (33)	C18 –C26-C17	113.24 (33)
C14' -C13'-C8'	115.18 (26)	C5 –C10-C6	120.82 (33)	C18 –C26-C19	108.37 (40)
C14' -C13'-C15'	104.23 (26)	C5 –C10-C4	120.82 (33)	C19 -C18-C20	115.81 (54)
C7' -C8'-C6'	112.63 (29)	C6' - C7' C5'	124.82 (32)	C21 -C20-C23	108.74 (86)
C13' -C14'-C25'	112.74 (28)	C3 -C2-O1	112.95 (30)	C21 -C22-C23	105.77 (93)
C13' -C12'-C25'	110.71 (29)	C3 –C4-O1	110.45 (32)	C21 -C22-C20	108.74 (86)
C13' -C17'-C25'	109.55 (28)	C3 –C4-C2	109.25 (29)	C20'-C21' -C19'	123.24 (66)
C13' -C12'-C14'	105.85 (26)	C12' -C13'- C11'	111.54 (27)	C22' -C21' -C27'	104.13 (1.62)

C23' -C28' -C29'	108.29 (79)
C23' -C21' -C29'	110.86 (59)
C23' -C21' -C28'	110.82 (68)
C21' -C22' -C20'	108.38 (74)
C21' -C23' -C20'	109.77 (60)
C21' -C23' -C22'	108.83 (75)
C20 -C21-C19	117.66 (71)
C22 -C21-C27	116.63 (1.34)
C23 -C28-C29	113.63 (1.17)
C23 -C28-C29	127.77 (1.21)
C23 -C28-C29	113.19 (98)

APPENDIX XIV (A): ^{1}H-NMR SPECTRUM OF DI-O-METHYL ISOOLIVIL

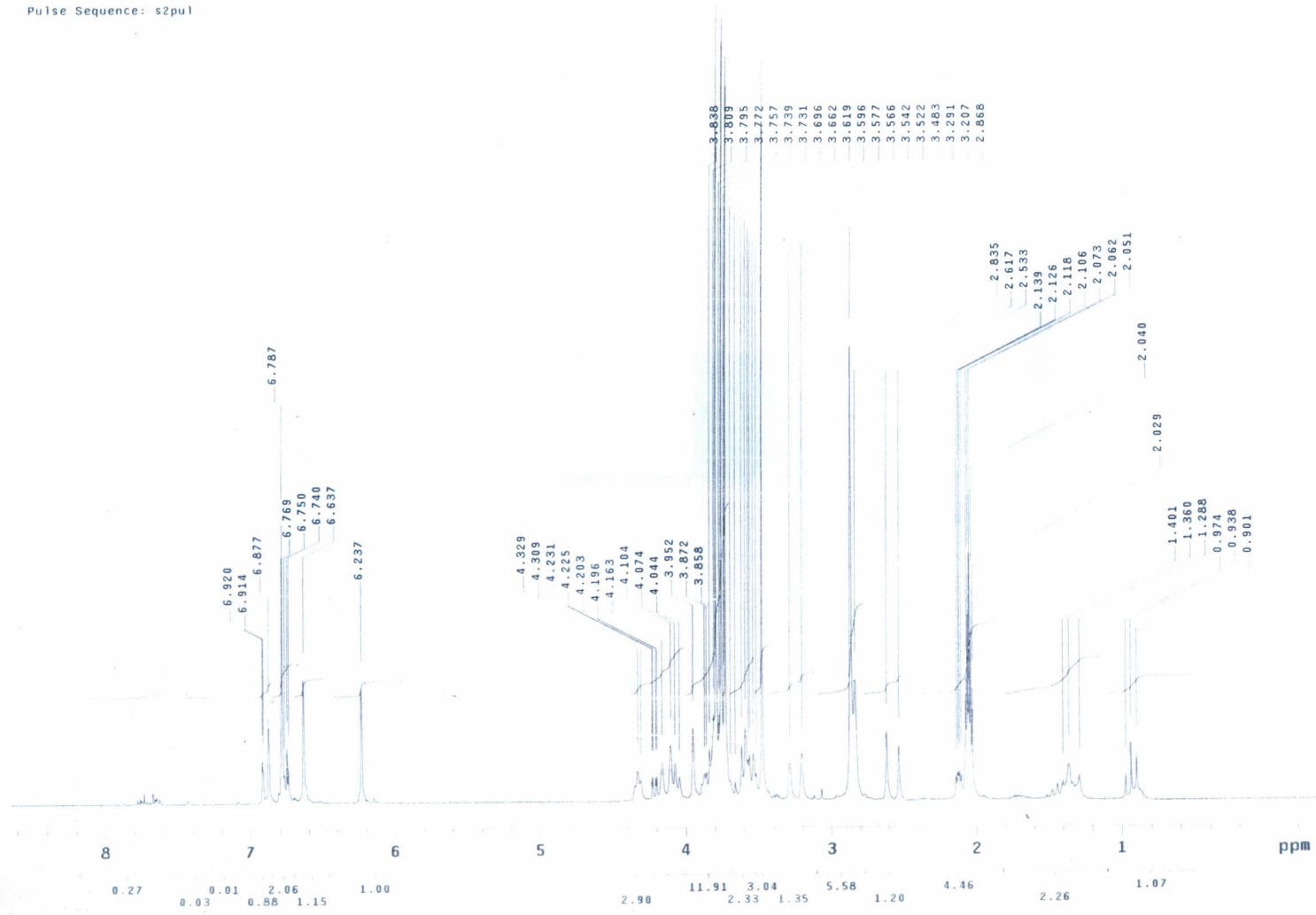

APPENDIX XIV (B): ^{1}H-NMR SPECTRUM OF [illegible]

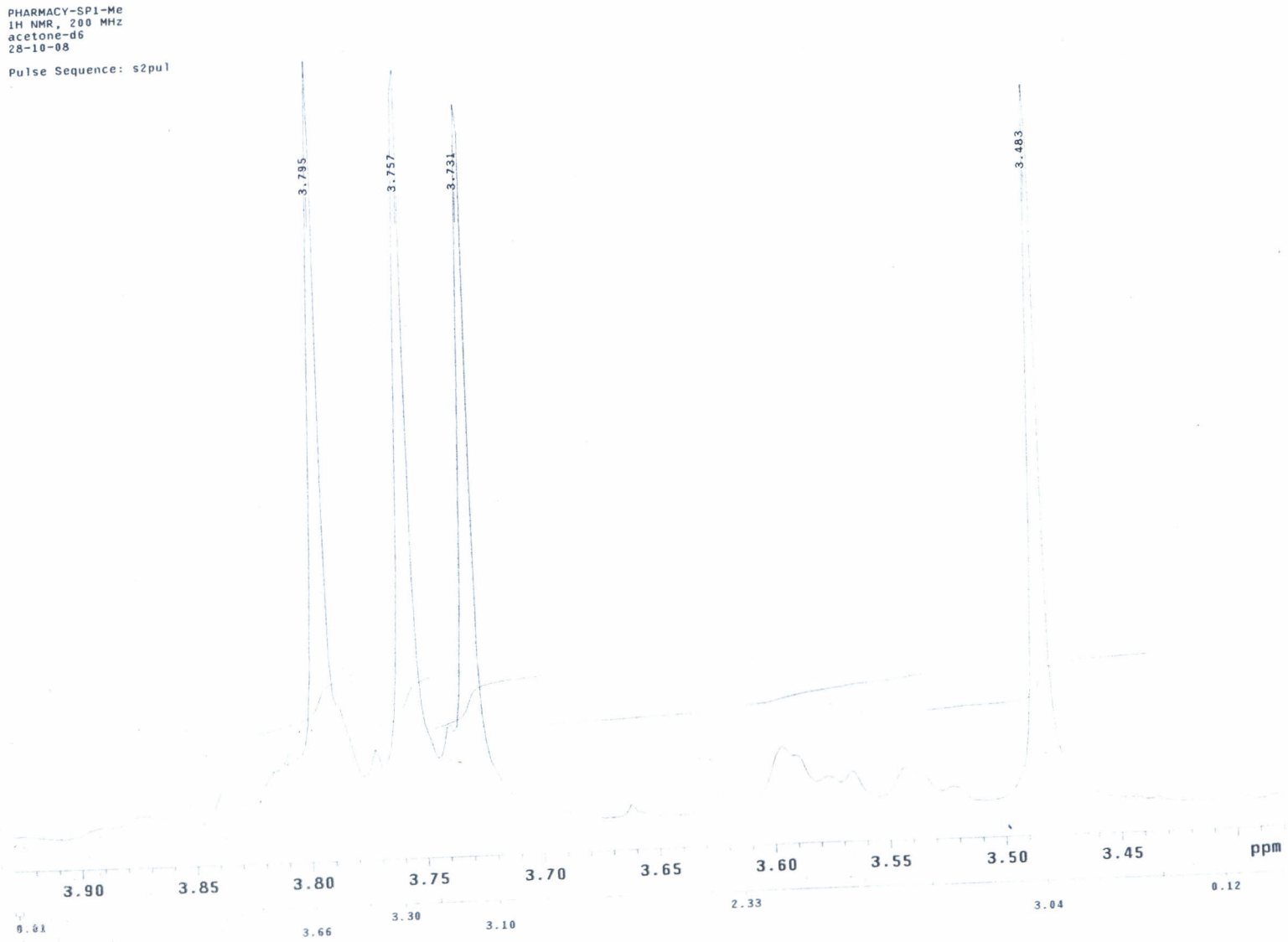

APPENDIX XV (A): C-NMR SPECTRUM OF DI-O-METHYL ISOCLIVIL

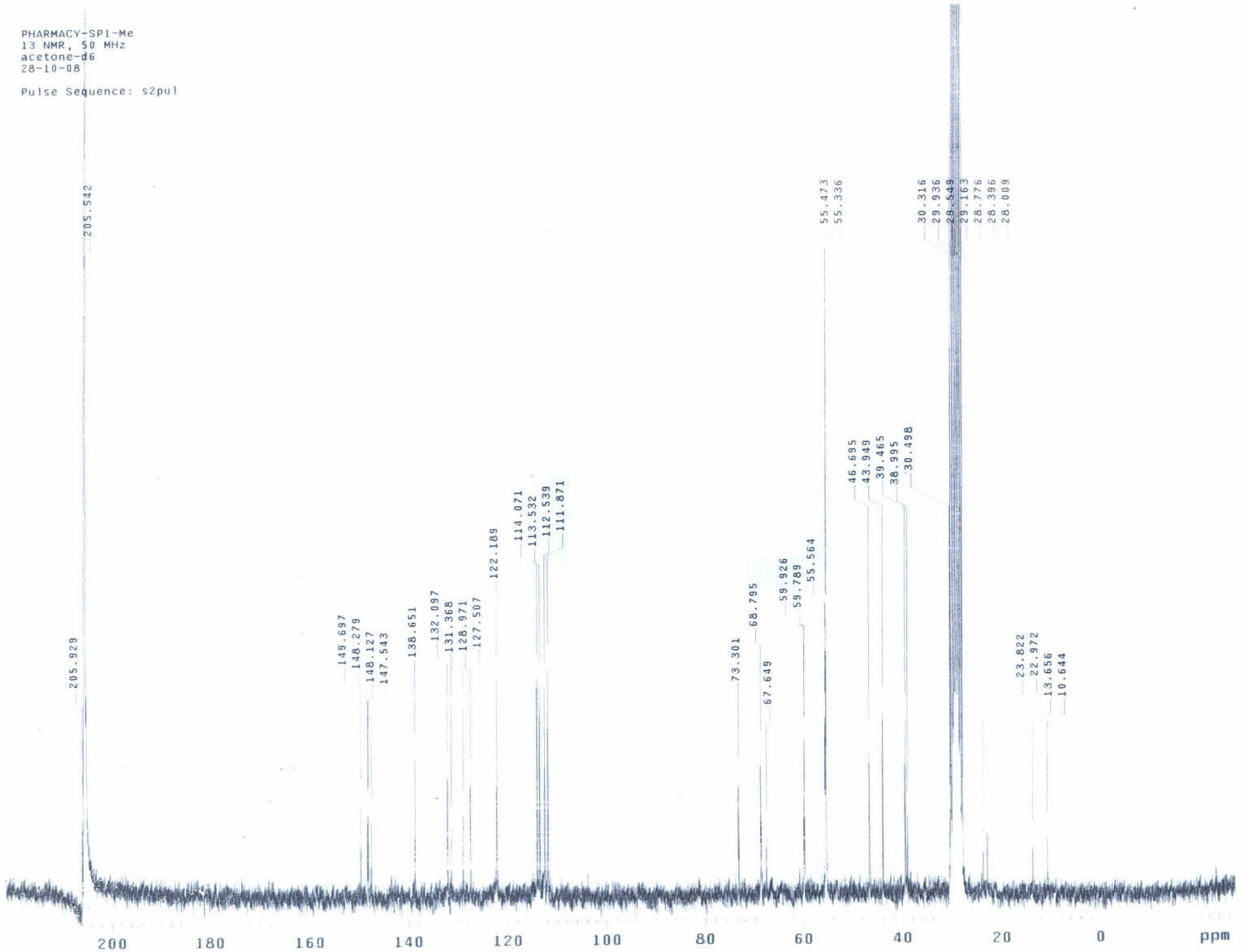

APPENDIX XV (B): ^{13}C-NMR SPECTRUM OF DI-O-METHYL ISOOLIVIL – METHOXY CARBONS